The Plant Cell, Vol. 17, 2296–2313, August 2005, www.plantcell.org © 2005 American Society of Plant Biologists

The Formin Homology 1 Domain Modulates the Actin Nucleation and Bundling Activity of Arabidopsis FORMIN1 [W]

Alphée Michelot,[a,1] Christophe Guérin,[a,1] Shanjin Huang,[b,1] Mathieu Ingouff,[a] Stéphane Richard,[c] Natalia Rodiuc,[a] Christopher J. Staiger,[b,2] and Laurent Blanchoin[a,2]

[a] Laboratoire de Physiologie Cellulaire Végétale, Commissariat à l'Energie Atomique, Centre National de la Recherche Scientifique, Institut National de la Recherche Agronomique, Université Joseph Fourier, Unité Mixte de Recherche 5168, F38054, Grenoble, France

[b] Department of Biological Sciences and Bindley Bioscience Center, Purdue University, West Lafayette, Indiana 47907-2064

[c] Salk Institute, Structural Biology Laboratory, La Jolla, California 92037

The organization of actin filaments into large ordered structures is a tightly controlled feature of many cellular processes. However, the mechanisms by which actin filament polymerization is initiated from the available pool of profilin-bound actin monomers remain unknown in plants. Because the spontaneous polymerization of actin monomers bound to profilin is inhibited, the intervention of an actin promoting factor is required for efficient actin polymerization. Two such factors have been characterized from yeasts and metazoans: the Arp2/3 complex, a complex of seven highly conserved subunits including two actin-related proteins (ARP2 and ARP3), and the FORMIN family of proteins. The recent finding that *Arabidopsis thaliana* plants lacking a functional Arp2/3 complex exhibit rather modest morphological defects leads us to consider whether the large FORMIN family plays a central role in the regulation of actin polymerization. Here, we have characterized the mechanism of action of Arabidopsis FORMIN1 (AFH1). Overexpression of AFH1 in pollen tubes has been shown previously to induce abnormal actin cable formation. We demonstrate that AFH1 has a unique behavior when compared with nonplant formins. The activity of the formin homology domain 2 (FH2), containing the actin binding activity, is modulated by the formin homology domain 1 (FH1). Indeed, the presence of the FH1 domain switches the FH2 domain from a tight capper (K_d ~3.7 nM) able to nucleate actin filaments that grow only in the pointed-end direction to a leaky capper that allows barbed-end elongation and efficient nucleation of actin filaments from actin monomers bound to profilin. Another exciting feature of AFH1 is its ability to bind to the side and bundle actin filaments. We have identified an actin nucleator that is able to organize actin filaments directly into unbranched actin filament bundles. We suggest that AFH1 plays a central role in the initiation and organization of actin cables from the pool of actin monomers bound to profilin.

INTRODUCTION

In plants, the cytoskeleton (i.e., microtubules and actin filaments) has long been known to play a major role in specialized functions during cell division, cell expansion and morphogenesis, or in response to pathogen attack (Staiger, 2000; Wasteneys and Galway, 2003; Staiger and Hussey, 2004; Wasteneys and Yang, 2004). Plant cells respond to a wide range of internal or external stimuli by reorganizing their cytoplasm (Vantard and Blanchoin, 2002). These modifications often correlate with changes in the actin filament network, suggesting a direct correlation between signal transduction and actin cytoskeleton reorganization in plants (Staiger and Hussey, 2004). Despite growing evidence that signal transduction cascades are required for plants to link signaling to the actin cytoskeleton, such signaling pathways have not yet been fully elucidated.

The elongation of the pollen tube is one of the best-characterized examples of actin-based cellular morphogenesis in plants (Hepler et al., 2001; Holdaway-Clarke and Hepler, 2003; Wasteneys and Galway, 2003). Fast pollen tube elongation (up to 1 cm/h for maize [*Zea mays*] pollen growing in vivo) allows fertilization of the ovule over a long distance in periods of <24 h. Actin is one of the most abundant proteins in pollen and plays a major role during tip growth (Yen et al., 1995; Ren et al., 1997; Staiger and Hussey, 2004). Any perturbation of the actin cytoskeleton by overexpression of actin binding proteins, drug treatments, or antibody injection into pollen induces morphological defects and often arrests tip growth (Lin and Yang, 1997; Gibbon et al., 1999; Vidali et al., 2001; Chen et al., 2002). However, how actin binding proteins are coordinated to ensure correct behavior of the actin cytoskeleton during pollen tube growth is an open debate.

A major long-standing challenge in plant biology is to understand how cells initiate actin filaments and thereby generate new actin filament arrays. Two main reasons argue against the spontaneous polymerization of actin filaments in plants. First, the need for precise spatial and temporal control over actin

[1] These authors contributed equally to this work.

[2] To whom correspondence should be addressed. E-mail cstaiger@bilbo.bio.purdue.edu or laurent.blanchoin@cea.fr; fax 765-496-1496 or 33-4-38785091.

The author responsible for distribution of materials integral to the findings presented in this article in accordance with the policy described in the Instructions for Authors (www.plantcell.org) is: Laurent Blanchoin (laurent.blanchoin@cea.fr).

[W] Online version contains Web-only data.

Article, publication date, and citation information can be found at www.plantcell.org/cgi/doi/10.1105/tpc.105.030908.

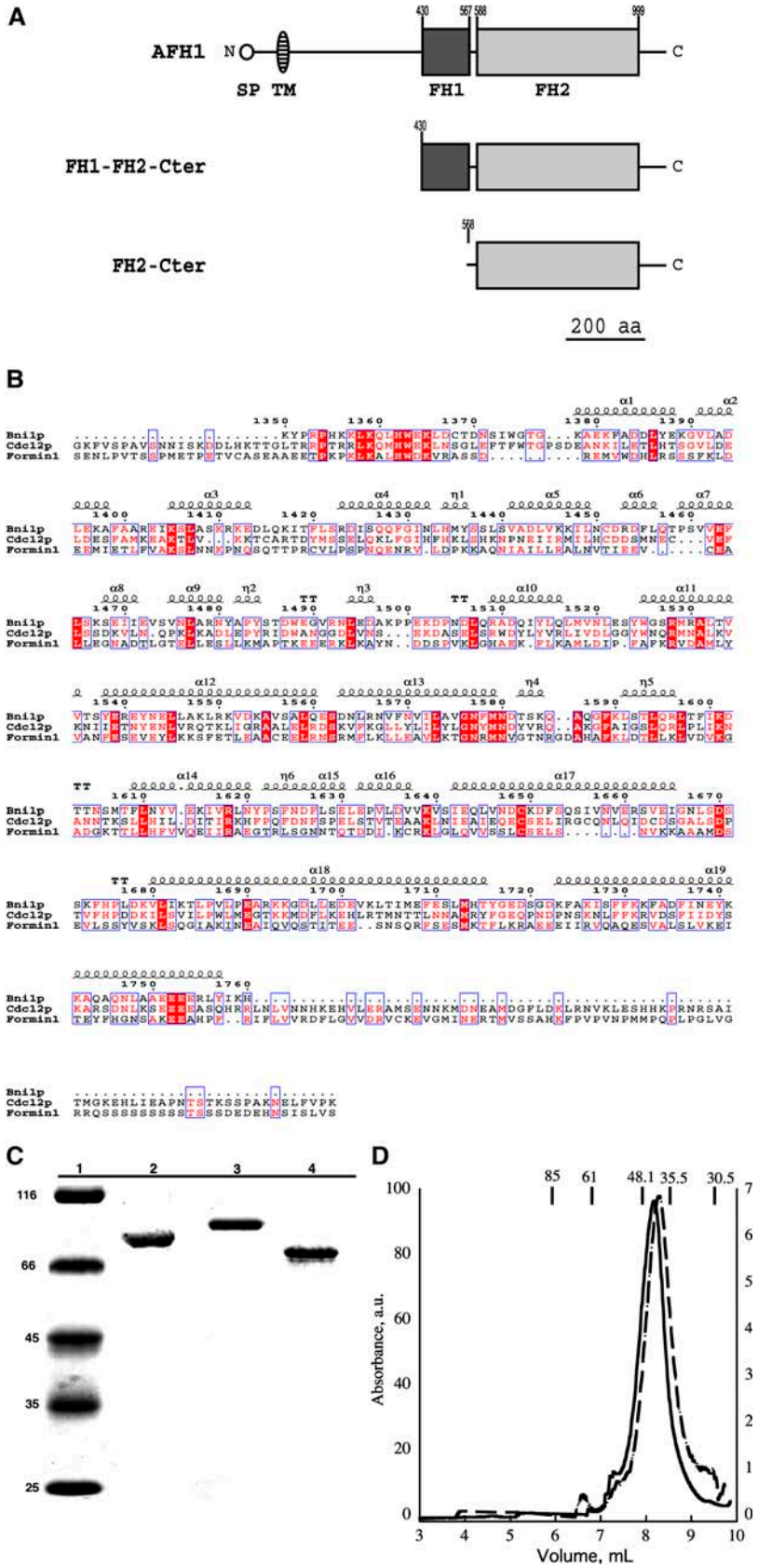

Figure 1. Purification of AFH1 and FH1-FH2-Cter and FH2-Cter Fusion Proteins.

polymerization in all cellular processes seems obvious. Indeed, cellular disruption of the equilibrium between actin monomers and actin filaments by overexpression of actin binding proteins or using actin cytoskeleton drugs (e.g., latrunculin or phalloidin) induces morphological and cytoarchitectural defects in plant cells (Staiger et al., 1994; Gibbon et al., 1999; Szymanski et al., 1999; Vidali et al., 2001). Second, the high in vivo concentration of profilin will buffer any free actin monomers and eliminate spontaneous formation of new filaments (Gibbon et al., 1997; Snowman et al., 2002; Staiger and Hussey, 2004). In fact, binding of profilin to ATP-actin monomers inhibits the formation of actin dimers or trimers, essential intermediates for the formation of actin filaments (Pollard et al., 2000).

The polymerization of actin in a plant cell, like other eukaryotes, will therefore require the intervention of actin-nucleating factors (Pollard et al., 2000; Staiger, 2000). Two actin-promoting factors are known: the Arp2/3 complex originally purified from *Acanthamoeba castellanii* (Machesky et al., 1994) and formins identified as a link between Cdc42p and the actin cytoskeleton during polarized morphogenesis in yeast (Evangelista et al., 1997). The Arp2/3 complex generates a branched network of actin filaments (Mullins et al., 1998), whereas formins induce polymerization of actin filaments organized into parallel cables (Feierbach and Chang, 2001; Evangelista et al., 2002; Sagot et al., 2002a). Analysis of the *Arabidopsis thaliana* genome reveals the presence of orthologs for all seven subunits of the Arp2/3 complex (Deeks and Hussey, 2003; Smith and Li, 2004). However, Arabidopsis plants defective in the expression of several of the subunits show morphological and cytological defects only in specialized cell types, including trichomes, leaf pavement cells, and root hairs (Li et al., 2002; Le et al., 2003; Mathur et al., 2003a, 2003b). One hypothesis arising from these surprising results is that actin polymerization in plant cells is mainly controlled by the large formin family (Wasteneys and Yang, 2004).

Formins are characterized by the presence of two different formin homology domains, formin homology domain 1 (FH1) and formin homology domain 2 (FH2), that allow the multiple activities of these proteins on actin (Pruyne et al., 2002; Sagot et al., 2002b; Kovar et al., 2003; Li and Higgs, 2003; Pring et al., 2003). In yeast, they are responsible for the formation of actin cables involved in both cell polarity and cytokinesis (Feierbach and Chang, 2001; Evangelista et al., 2002; Sagot et al., 2002a). Biophysical approaches show that for yeast and mammalian formins, the FH2 domain contains the actin binding site, whereas FH1 with its polyproline-rich stretches binds to profilin and the profilin/actin complex (Pruyne et al., 2002; Sagot et al., 2002b; Li and Higgs, 2003). General features of all formins include the abilities to nucleate actin filaments, to interact with the barbed end of actin filaments, and to allow actin elongation at the barbed end while remaining attached to the same end (Pruyne et al., 2002; Sagot et al., 2002b; Kovar et al., 2003; Li and Higgs, 2003; Higashida et al., 2004; Kovar and Pollard, 2004a; Romero et al., 2004). The latter behavior led to the elaboration of a model where formin acts as a processive actin-promoting factor (Pruyne et al., 2002; Zigmond et al., 2003). However, a detailed analysis of the literature on formins reveals a wide range of effects on actin polymerization (Pruyne et al., 2002; Sagot et al., 2002b; Kovar et al., 2003; Li and Higgs, 2003; Zigmond et al., 2003; Harris et al., 2004; Romero et al., 2004). This is probably due to the multiple synergistic or antagonist reactions that formin has on actin polymerization (Kovar and Pollard, 2004b).

Arabidopsis has 21 FORMIN isoforms separated into two distinct phylogenetic subfamilies (Cvrcková, 2000; Deeks et al., 2002; Cvrcková et al., 2004). Class I is characterized by a predicted N-terminal transmembrane domain that partially targets the formin to or near the plasma membrane (Cheung and Wu, 2004; Favery et al., 2004; Van Damme et al., 2004; Ingouff et al., 2005). No data are yet available for class II. Overexpression of Arabidopsis FORMIN1 (AFH1) in pollen tubes induces the formation of prominent actin cables, pollen tube swelling, and deformation of the cell membrane at the tip of the pollen tube (Cheung and Wu, 2004). The complexity of formin activities makes predictions about the mechanisms underlying the broad effects seen on pollen tubes rather impractical. The yeast and mammalian cell biologists have expended considerable effort toward better understanding of the mechanisms of action of formin in vitro, whereas limited comparable data are yet available for plant formins (Ingouff et al., 2005). A detailed analysis of the mechanism of action of AFH1 is urgently needed before going any further in the understanding of its in vivo functions.

Here, we combined pyrene fluorescence and light scattering assays of actin polymerization, together with direct visualization

Figure 1. (continued).

(A) Schematic representation of the predicted domain organization of AFH1. The FH1 domain is dark gray (amino acids 430 to 567), and the FH2 domain is light gray (amino acids 588 to 999). Recombinant FH1-FH2-Cter and FH2-Cter fusion proteins include amino acids 430 to 1051 and 568 to 1051, respectively. SP, signal peptide, TM, transmembrane domain; aa, amino acids.

(B) Sequence alignment of AFH1 FH2-Cter domain with the equivalent domain of fission yeast Cdc12p and budding yeast Bni1p, based on the structure of FH2 domain of Bni1p (Xu et al., 2004). Multiple sequence alignment of the AFH1 domain with the *Saccharomyces cerevisiae* Bni1p FH2 domain and the *Schizosaccharomyces pombe* cytokinesis formin Cdc12p sequences was done with MultAlin (http://prodes.toulouse.inra.fr/multalin/). Superimposition with the secondary structures extracted from the Bni1p crystal structure (Protein Data Bank ID 1UX5) was done with EsPript (http://espript.ibcp.fr/ESPript/ESPript/). Numbering is based on the Bni1p crystal structure (1UX5).

(C) Coomassie-stained 10.5% SDS-PAGE of purified recombinant formin proteins after purification by affinity chromatography on glutathione-Sepharose followed by nickel-Sepharose for GST-AFH1-His constructs or by nickel-Sepharose only for His-AFH1-His construct. Lane 1, molecular weight markers in kD; lane 2, GST-FH2-Cter-His protein; lane 3, GST-FH1-FH2-Cter-His protein; lane 4, His-FH1-FH2-Cter-His protein.

(D) Analytical gel filtration analysis of AFH1, FH1-FH2-Cter constructs. Peak elution volumes for the following markers are shown along the top: 85 Å = thyroglobulin; 61 Å = ferritin; 48.1 Å = aldolase; 35.5 Å = BSA; 30.5 Å = ovalbumin. AFH1 GST-FH1-FH2-Cter-His elutes at 8.15 mL (solid line), corresponding to a Stokes radius of 41.2 Å, and His-FH1-FH2-Cter-His elutes at 8.3 mL (dashed line), corresponding to an apparent Stokes radius of 39.7 Å. a.u., arbitrary absorbance units.

of actin filaments at steady state by fluorescence microscopy or during polymerization by evanescent wave microscopy, to analyze the effect of AFH1 on actin dynamics. We demonstrate that recombinant FH2-Cter and FH1-FH2-Cter (the isolated FH1 and FH2 domains) were both able to accelerate polymerization of actin alone; however, the FH1 domain was essential for effective nucleation of actin monomers bound to profilin. This plant actin binding protein is able to use the pool of actin monomers bound to profilin for efficient nucleation. FH2-Cter and FH1-FH2-Cter domains of AFH1 interact with the barbed ends of actin filaments, inhibiting end-to-end annealing, but their effect on barbed-end dynamics is very different and unique when compared

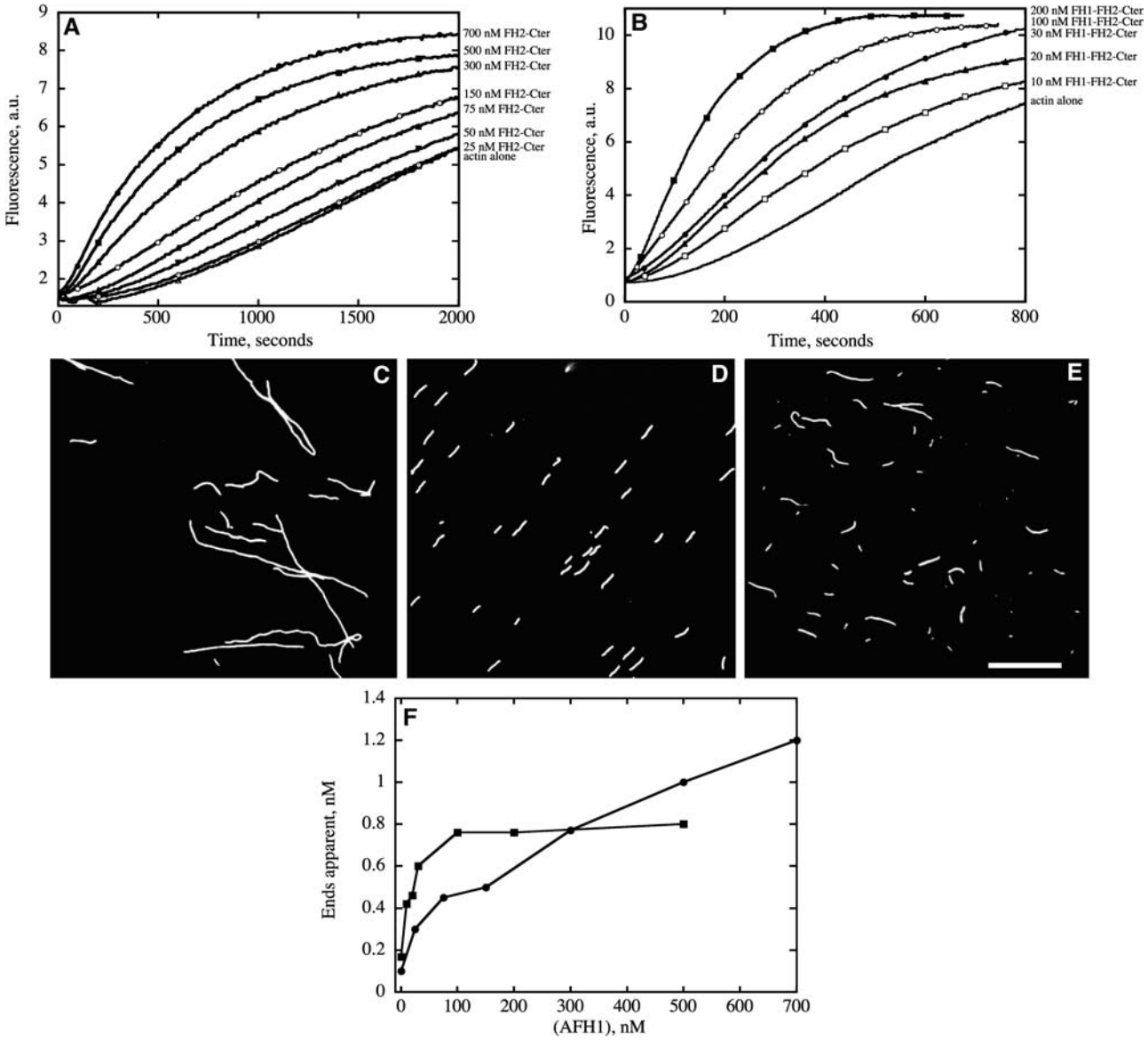

Figure 2. FH2-Cter and FH1-FH2-Cter Nucleate Actin Polymerization.

Conditions: 10 mM imidazole-HCl, pH 7.0, 50 mM KCl, 1 mM $MgCl_2$, 1 mM EGTA, 0.2 mM ATP, 0.2 mM $CaCl_2$, 0.5 mM DTT, and 3 mM NaN_3 at 20°C.
(A) Time course of actin polymerization in the presence of FH2-Cter monitored by pyrene fluorescence. Different concentrations of FH2-Cter were added to 2 μM of 10% pyrene-labeled actin before initiation of polymerization.
(B) Time course of actin polymerization in the presence of FH1-FH2-Cter. Increasing amounts of FH1-FH2-Cter were added to 4 μM of 10% pyrene-labeled actin before initiation of polymerization.
(C) to **(E)** Micrographs of actin filaments in the presence of AFH1. Actin alone **(C)**, actin and 700 nM FH2-Cter **(D)**, and actin and 200 nM FH1-FH2-Cter **(E)**. Bar in **(E)** = 5 μm.
(F) Nucleation efficiency of FH2-Cter and FH1-FH2-Cter. The efficiency of nucleation for FH2-Cter (closed circles) and FH1-FH2-Cter (closed squares) was determined at half-maximal polymerization according to Blanchoin et al. (2000b).

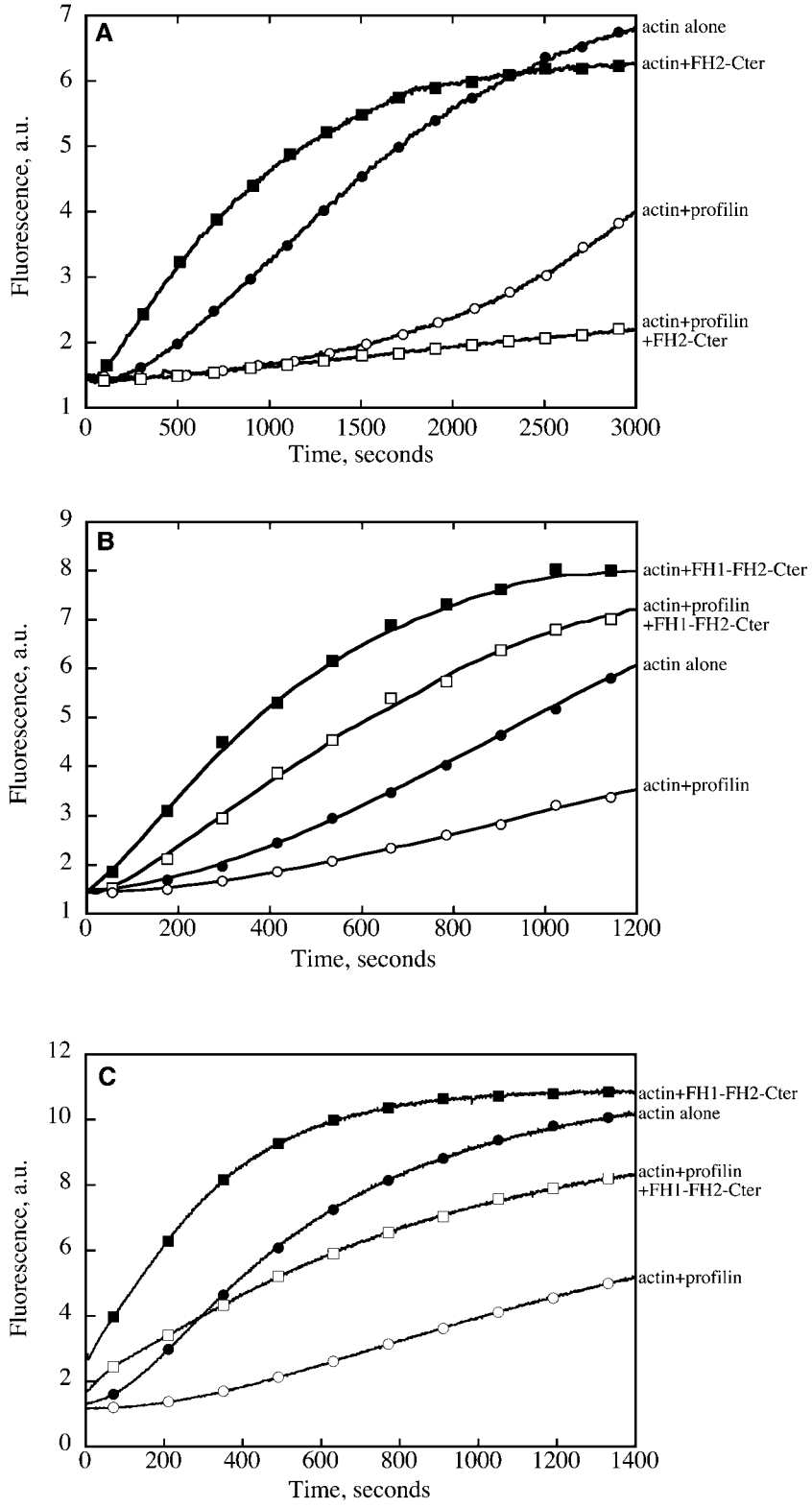

Figure 3. The FH1 Domain Is Necessary for Efficient Nucleation of Profilin/Actin Complex by AFH1.

Conditions: 10 mM imidazole, pH 7.0, 50 mM KCl, 1 mM $MgCl_2$, 1 mM EGTA, 0.2 mM ATP, 0.2 mM $CaCl_2$, 0.5 mM DTT, and 3 mM NaN_3 at 20°C.
(A) Time course of actin polymerization in the presence of FH2-Cter and profilin monitored by pyrene fluorescence. Actin alone at 2 μM, closed circles;

with nonplant formins. The FH2-Cter domain acts like an efficient capper and blocks elongation at the barbed end of actin filaments. However, the presence of the FH1 domain allows the FH1-FH2-Cter protein to bind the barbed ends and allow elongation at the barbed ends. More surprising, the FH1-FH2-Cter protein was able to bind to the side and bundle actin filaments directly. We report an actin nucleator that is able to organize actin filaments into unbranched actin filament bundles. These data strongly support a key role of AFH1 in the initiation and organization of actin cables from the pool of actin monomers bound to profilin.

RESULTS

Generation of Recombinant FH2-Cter and FH1-FH2-Cter Domains of AFH1

To characterize the mechanism of action of AFH1, we generated two C-terminal constructs containing the actin binding activity, FH2-Cter, and FH1-FH2-Cter, including amino acids 568 to 1051 and 430 to 1051, respectively (Figure 1A). A sequence comparison between FH2-Cter of yeast formins Bni1p, Cdc12p, and AFH1 reveals that AFH1 shares ~25% similarity with both proteins and has a Ser-rich extension of 46 amino acids at the C-terminal end (Figure 1B). The FH1 domain amino acids (430 to 567) contain a typical polyproline-rich stretch, implicated in binding to profilin (Evangelista et al., 1997; Watanabe et al., 1997; Banno and Chua, 2000), but shares low similarity with other formin FH1 domains. We expressed in bacteria both constructs of AFH1 with a glutathione *S*-transferase (GST) fusion at the N terminus and a 6-His tag at the C terminus (Figure 1C). Cleavage of GST from either construct induced a rapid degradation of the proteins. Because no differences in nucleation activity between GST-tagged and untagged proteins were detected, we used GST fusions for the bulk of our studies. To rule out the possibility of GST dimer formation, which might be responsible for the bundling activity observed with GST-FH1-FH2-Cter protein, we made recombinant FH1-FH2-Cter with a 6-His tag at both N and C termini (Figure 1C). Using analytical gel filtration, we compared the elution profiles of the two FH1-FH2-Cter proteins. Both proteins behaved similarly and eluted with an apparent Stokes radius at the peak of 41.2 and 39.7 Å, consistent with a spherical particle of 107 kD for GST-FH1-FH2-Cter-His and 96.7 kD for His-FH1-FH2-Cter-His. These values are slightly greater than the masses calculated for the monomers, 96.5 and 68.5 kD, respectively (Figure 1D). These proteins eluted as a broad peak, suggesting that they exist probably in a monomer-dimer equilibrium.

FH2-Cter and FH1-FH2-Cter Proteins Nucleate Actin Polymerization

We used a combination of pyrene-actin assays and direct visualization of actin filaments by light microscopy to study the effect of FH2-Cter and FH1-FH2-Cter on actin polymerization (Figures 2A to 2E). In pyrene fluorescence, both FH2-Cter and FH1-FH2-Cter proteins decreased the initial lag corresponding to the nucleation step for actin polymerization in a concentration-dependent manner (Figures 2A and 2B). The behavior of AFH1 FH2-Cter is distinct from the equivalent fusion protein AtFH5, which does not nucleate actin from a pool of free actin monomers (Ingouff et al., 2005). The amplitude of pyrene fluorescence at steady state, which is directly proportional to the actin filament concentration generated during polymerization, was only slightly affected by the presence of AFH1 FH1-FH2-Cter fusion protein. This suggests that this protein does not change the final polymer concentration during polymerization. Because the mean length of actin filaments is inversely proportional to the number of nuclei generated during the polymerization, we used light microscopy to determine directly the length of actin filaments generated at the end of actin polymerization in the presence of AFH1 fusion proteins. The presence of either protein in the polymerization mixture before dilution and observation in the light microscope showed a decrease in the mean size of actin filaments from 18 μm for actin alone to 3.4 and 3.7 μm for FH2-Cter (700 nM) and FH1-FH2-Cter (200 nM), respectively, in agreement with pyrene fluorescence polymerization curves (Figures 2C to 2E).

The FH1 Domain Is Necessary for Actin Filament Nucleation from the Profilin/Actin Complex

It has been reported for some plant cells that a large pool of unpolymerized actin is buffered by a high concentration of profilin (Gibbon et al., 1999; Snowman et al., 2002; Staiger and Hussey, 2004). It was imperative to test whether or not AFH1 is able to use this large pool of actin bound to profilin for efficient nucleation of actin filaments. We first tested the effect of FH2-Cter on the polymerization of actin/profilin complex. The presence of an equimolar amount of profilin to actin inhibited the polymerization of actin by increasing the lag corresponding to the nucleation step (Figure 3A, open circles, compared with actin alone, closed circles). FH2-Cter was able to nucleate polymerization of actin alone (Figure 3A, closed squares). However,

Figure 3. (continued).

2 μM actin with 2 μM profilin, open circles; 2 μM actin with 300 nM FH2-Cter, closed squares; 2 μM actin with 2 μM profilin and 300 nM FH2-Cter, open squares.

(B) Time course of actin polymerization in the presence of FH1-FH2-Cter and profilin monitored by pyrene fluorescence. Actin alone at 2 μM, closed circles; 2 μM actin with 2 μM profilin, open circles; 2 μM actin with 50 nM FH1-FH2-Cter, closed squares; 2 μM actin with 2 μM profilin and 50 nM FH1-FH2-Cter, open squares.

(C) Time course of maize actin polymerization in the presence of FH1-FH2-Cter and maize profilin (ZmPRO5) monitored by pyrene fluorescence. Actin alone at 2 μM, closed circles; 2 μM actin with 2 μM profilin, open circles; 2 μM actin with 100 nM FH1-FH2-Cter, closed squares; 2 μM actin with 2 μM profilin and 100 nM FH1-FH2-Cter, open squares.

polymerization was fully inhibited in the presence of both FH2-Cter and equimolar profilin to actin (Figure 3A, open squares). By contrast, FH1-FH2-Cter was able to nucleate actin alone (Figure 3B, closed squares) and profilin/actin complex (Figure 3B, open squares). Similar results were obtained when we replaced human profilin and muscle actin with maize profilin and pollen actin (Figure 3C). FH1-FH2-Cter was able to nucleate both pollen actin (Figure 3C, closed squares) and pollen actin bound to maize profilin (Figure 3C, open squares).

FH2-Cter Blocks Elongation at the Barbed Ends Similar to Capping Protein

The profilin/actin complex can add only onto uncapped filament barbed ends (Pollard et al., 2000). A possible explanation for the inhibition of actin polymerization in the presence of FH2-Cter and profilin/actin is that FH2-Cter blocks elongation at actin filament barbed ends (Xu et al., 2004; Otomo et al., 2005). To investigate this hypothesis, seeded filament elongation experiments were performed. These assays used actin filaments alone or in the presence of FH2-Cter, as seeds for elongation with a concentration of pyrene-labeled actin monomers that were below the critical concentration (Cc) at the pointed ends (i.e., 0.7 μM). Under these conditions, elongation occurs only at the barbed ends. The initial rate of elongation is then directly proportional to the concentration of free barbed ends. We found, as expected, that 0.4 μM pyrene-actin monomers could elongate the F-actin seeds (Figure 4, open squares). By contrast, elongation of 0.4 μM pyrene-labeled actin monomers was strongly inhibited in the presence of FH2-Cter (Figure 4, closed circles) similar to the

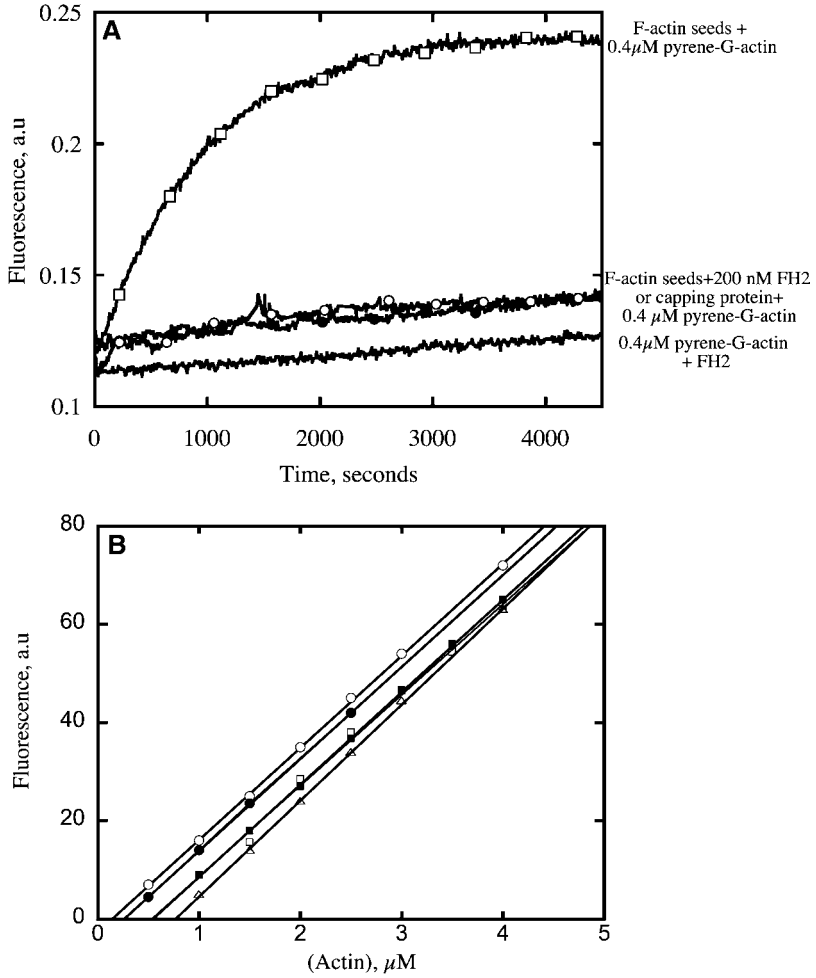

Figure 4. FH2-Cter Blocks Elongation at the Barbed Ends of Actin Filaments and Shifts the Cc to the Value for Pointed-End Assembly.

Conditions: 10 mM imidazole-HCl, pH 7.0, 50 mM KCl, 2 mM $MgCl_2$, 1 mM EGTA, 0.2 mM ATP, 0.2 mM $CaCl_2$, 0.5 mM DTT, and 3 mM NaN_3 at 20°C.
(A) Time course of 0.4 μM pyrene-labeled actin elongation from a reaction mixture of 1 μM unlabeled actin filaments alone (open squares), 1 μM unlabeled actin filaments preincubated with 200 nM FH2-Cter (closed circles), or 1 μM unlabeled actin filaments preincubated with 200 nM capping protein (AtCP; open circles). Control for the effect of 200 nM FH2-Cter on the polymerization of 0.4 μM pyrene-labeled actin (solid line).
(B) Effect of FH2-Cter and FH1-FH2-Cter proteins on the Cc. Dependence of actin polymer concentration on total actin concentration in the absence (open circles; Cc = 0.14 μM) or presence of 200 nM FH1-FH2-Cter (closed circles; Cc = 0.24 μM), 200 nM FH2-Cter (closed squares; Cc = 0.54 μM), 200 nM AtCP (open squares; Cc = 0.59 μM), or 200 nM human gelsolin (open triangles; Cc = 0.76 μM).

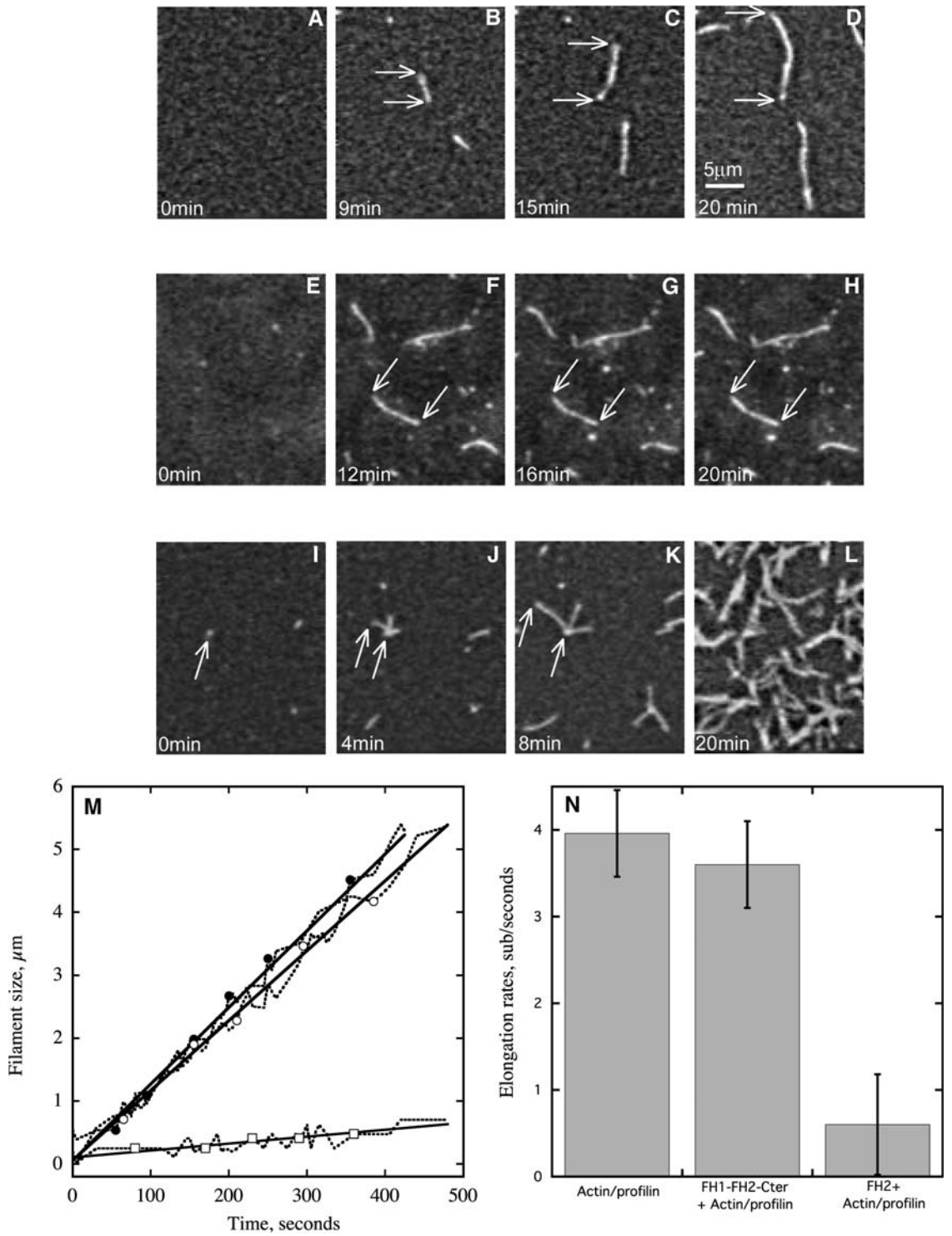

Figure 5. Direct Visualization by TIRF Microscopy of the Effect of FH2-Cter or FH1-FH2-Cter on Actin Filament Elongation by Profilin/Actin Complex.

(A) to **(D)** Time lapse evanescent wave fluorescence microscopy of profilin/rhodamine-actin polymerization. Conditions: NEM-myosin was attached to the cover glass before addition into the flow cell of profilin/rhodamine-actin complex (2 and 1 μM, respectively). Frames were taken at the indicated time during polymerization. Bar = 5 μm.

(E) to **(H)** Time lapse evanescent wave fluorescence microscopy of the effect of FH2-Cter on actin polymerization. Conditions: NEM-myosin and FH2-Cter (500 nM) were attached to the cover glass before addition into the flow cell of profilin/rhodamine-actin complex (2 and 1 μM, respectively). Frames were taken at the indicated time during polymerization.

effect of Arabidopsis capping protein, a protein known to block barbed-end elongation (Huang et al., 2003) (Figure 4, open circles).

We next investigated the effect of both FH2-Cter and FH1-FH2-Cter proteins on the Cc for actin assembly. The FH2-Cter construct increased the Cc from 0.14 μM for actin filament (Figure 4B, open circles) with free barbed ends to 0.54 μM, a value close to that for the Cc of the pointed ends (Figure 4B, closed squares). Arabidopsis capping protein (Cc = 0.59 μM; Figure 4, open squares) or human gelsolin (Cc = 0.76 μM; Figure 4B, open triangles) had similar effects. However, the FH1-FH2-Cter construct has only a slight effect on the Cc (Cc = 0.24 μM; Figure 4B, closed circles). These results suggest that the presence of the FH1 domain modulates the behavior of the FH2-Cter domain at the barbed end of actin filaments.

To further confirm this hypothesis, we used a total internal reflection fluorescence (TIRF) microscope assay designed by Kovar and Pollard (2004a). In this assay, both *N*-ethylmaleimide (NEM)-myosin and FH2-Cter or FH1-FH2-Cter were immobilized on the cover glass of a flow cell before addition of rhodamine-actin/profilin complex to monitor polymerization (Figure 5). NEM-myosin is necessary in this assay to maintain actin filaments in the focal plane of the evanescent wave of illumination. The design of the assay and use of the TIRF microscope allowed us to distinguish two types of events: first, the polymerization in the volume of the flow cell where no AFH1 is present; second, the polymerization at the cover glass where both NEM-myosin and AFH1 are present. We were mostly interested in the elongation events at the cover glass because these are more likely to have filaments with AFH1 bound at the barbed end. In the presence of FH2-Cter (500 nM), actin filaments that were attached to NEM-myosin and visible in the TIRF focal plane (100 to 150 nm from the glass) were able to elongate over a period of 20 min at a very slow rate of 0.6 ± 0.6 subunits per second (see Supplemental Movie 2 online; Figures 5E to 5H, open squares in 5M, and 5N). However, in the absence of FH2-Cter (see Supplemental Movie 1 online; Figures 5A to 5D) or in the presence of FH1-FH2-Cter (see Supplemental Movie 3 online; Figures 5I to 5L), actin filaments at the cover glass were able to elongate several microns during the 20-min observation period. Only filaments attached by one end were measured to determine the rate of elongation in the presence of FH1-FH2-Cter construct to be sure that these filaments have a formin attached. The rates of elongation were 4 ± 0.5 subunits per second for profilin/actin complex alone (Figures 5M, closed circles, and 5N) or 3.5 ± 0.5 subunits per second for profilin/actin complex in the presence of FH1-FH2-Cter (Figures 5M, open circles, and 5N). This is in perfect agreement with the elongation and the Cc data (Figures 4A and 4B) and confirms that FH2-Cter blocks elongation at the barbed ends of actin filaments. According to these observations, we were then able to determine the nucleation efficiency of both constructs using the slope at half-maximal polymerization from the pyrene fluorescence curves (Figures 2A and 2B; Blanchoin et al., 2000b) using a rate constant of association 10 $\mu M^{-1}\,s^{-1}$ for FH1-FH2-Cter (i.e., rate constant for barbed-end elongation) and 1.3 $\mu M^{-1}\,s^{-1}$ for FH2-Cter (i.e., rate constant for pointed end elongation) (Figure 2F). FH1-FH2-Cter generates a maximum of 0.026 filament barbed ends per formin molecule (Figure 2F). This is 10 times more efficient than the equivalent fusion protein for AtFH5, about the same efficiency as Bni1p, but 10 times less efficient than mDia1 or Cdc12p (Sagot et al., 2002b; Kovar et al., 2003; Li and Higgs, 2003; Ingouff et al., 2005).

The Presence of the FH1 Domain Switches the FH2-Cter Protein from a Strong Capper to a Leaky Capper

Actin filament elongation assays (Blanchoin et al., 2000a) were used to determine the affinity of FH2-Cter and FH1-FH2-Cter for the barbed end of actin filaments (Figure 6). Freshly prepared seeds consisting of unlabeled actin filaments were incubated with various concentrations of FH2-Cter (Figure 6A) or FH1-FH2-Cter (data not shown) before addition of pyrene-labeled actin monomers. The decrease in the initial rate of elongation as a function of the concentration of AFH1 reflects the saturation of filament barbed ends by AFH1 fusion proteins (Figure 6B). Under these experimental conditions, the nucleation activity of both proteins at their highest concentrations did not contribute to the increase in the pyrene fluorescence signal (data not shown). We determined apparent K_d values of 3.7 ± 1.5 nM for FH2-Cter (Figure 6B, closed circles) and 40 ± 12 nM for FH1-FH2-Cter binding to muscle actin filament barbed ends (Figure 6B, open squares). The latter value is consistent with that measured for FH1-FH2-Cter from AtFH5 (K_d ~32 nM; Ingouff et al., 2005). A K_d of 3.1 ± 0.4 nM for FH2-Cter binding to pollen actin filament barbed ends (Figure 6B, open circles) confirmed that the source of actin does not affect AFH1 properties. Moreover, we found that binding of FH1-FH2-Cter to barbed ends decreased the rate of actin filament elongation, but unlike the FH2-Cter construct did not fully block elongation at the barbed ends (Figure 6B, open squares) in agreement with the Cc experiments (Figure 4B).

We reported previously that interaction of capping protein (CP) with the barbed end of actin filaments inhibits annealing of mechanically sheared actin filaments (Andrianantoandro et al., 2001; Huang et al., 2003). By wide-field fluorescence microscopy, we visualized the products of shearing a mixture of two colors of actin filaments directly (Figure 7). Ten seconds after

Figure 5. (continued).

(I) to **(L)** Time lapse evanescent wave fluorescence microscopy of the effect of FH1-FH2-Cter on actin polymerization. Conditions: NEM-myosin and FH1-FH2-Cter (200 nM) were attached to the cover glass before addition into the flow cell of profilin/rhodamine-actin complex (2 and 1 μM, respectively). Frames were taken at the indicated time during polymerization. Arrows indicate the position of actin filament ends over time.

(M) Measurement of filament length changes over time. Dotted lines represent actin filament elongation for a single actin filament in the absence (closed circles) or presence of FH1-FH2-Cter (open circles) or FH2-Cter (open squares). Linear fits (solid line) allow determination of the elongation rate.

(N) Bar graphs comparing elongation rates of filaments in the absence or presence of FH1-FH2-Cter or FH2-Cter.

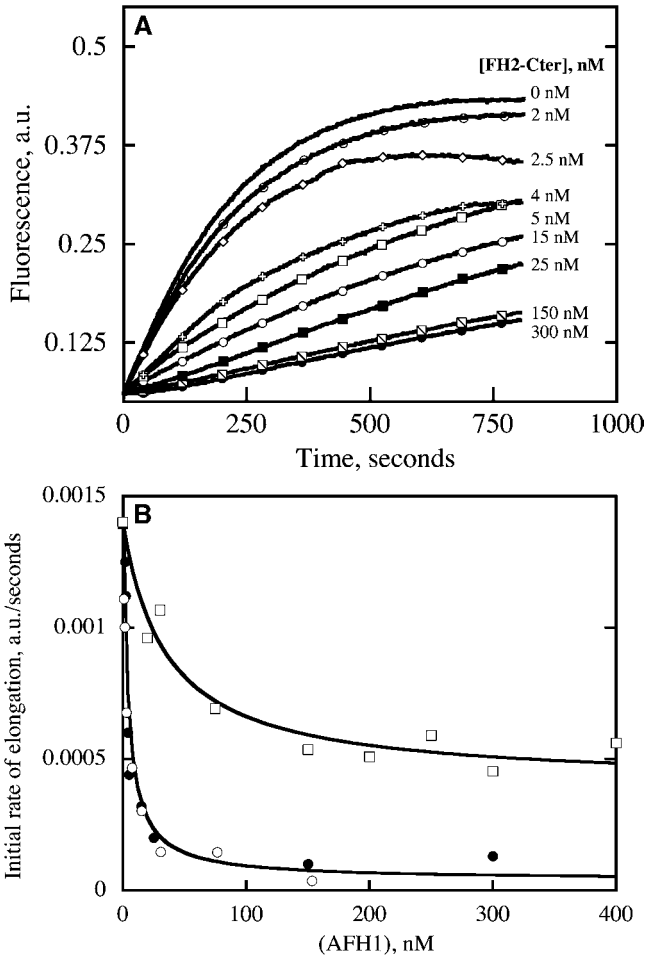

Figure 6. FH2-Cter Binds with a Higher Affinity to the Barbed Ends of Actin Filaments Than Does FH1-FH2-Cter.

(A) Kinetics of actin filament barbed-end elongation in the presence of FH2-Cter. Preformed actin filaments (1 μM) were incubated with various concentrations of FH2-Cter before addition of 1 μM pyrene-actin monomers.

(B) Variation in the initial rate of elongation as a function of FH2-Cter or FH1-FH2-Cter concentration. The data were fit with Equation 1 (see Methods) to determine equilibrium dissociation constant values of 3.7 nM for FH2-Cter (closed circles) with muscle actin, 40 nM for FH1-FH2-Cter (open squares) with muscle actin, and 3.1 nM for FH2-Cter (open circles) with pollen actin.

fragmentation, most of the filaments were very short (Figure 7A; mean length = 1.5 μm). Ten minutes after fragmentation, long actin filaments consisting of alternating red and green segments were formed by end-to-end annealing of the two original populations of filaments (Figures 7B and 7E; mean length = 5.7 μm). Incubation of actin filaments with 100 nM FH2-Cter before fragmentation inhibited the annealing reaction (Figures 7C and 7E; mean length = 1.2 μm). However, incubation with 100 nM FH1-FH2-Cter had only a slight effect on annealing (Figures 7D and 7E; mean length = 4.1 μm). Increasing the concentration of both FH2-Cter and FH1-FH2-Cter to 500 nM strongly inhibited annealing (Figure 7E, mean length = 0.5 μm), demonstrating that both proteins interact with the barbed ends of actin filaments but with a different affinity.

CP and FH1-FH2-Cter Compete for Binding to the Barbed End of Actin Filaments

It has been reported recently that the heterodimeric Arabidopsis CP binds to the barbed end of actin filaments with high affinity (K_d ~12 to 24 nM) and blocks elongation with profilin/actin complex (Huang et al., 2003). We investigated how CP affects filament nucleation from profilin/actin complexes by FH1-FH2-Cter using the pyrene fluorescence assay (Figure 8). CP decreased the nucleation efficiency of FH1-FH2-Cter in a concentration-dependent manner (Figure 8). In the presence of equimolar CP and FH1-FH2-Cter protein, nucleation was completely inhibited (Figure 8, closed squares). This demonstrates that CP and FH1-FH2-Cter have antagonist effects at the barbed end of actin filaments.

FH1-FH2-Cter Induces Bundling of Actin Filaments

During the fluorescence light microscopy assays, we discovered that FH1-FH2-Cter was able to organize individual actin filaments (Figure 9A) into long actin bundles (Figure 9C) similar to actin filament bundles observed in the presence of Arabidopsis VILLIN1, a well-characterized plant actin filament bundler (Figure 9B; Huang et al., 2005). No bundles were observed in absence of either VILLIN1 or FH1-FH2-Cter (Figure 9A). Bundling activity by a formin was originally reported for mouse formin FRLα (H. Rouiller, D. Hanein, and Harry Higgs, unpublished data). To further characterize the bundling activity of FH1-FH2-Cter, we performed a side by side low-speed cosedimentation assay with this protein and VILLIN1 (Figures 9D and 9E). At low speed, actin filaments and FH1-FH2-Cter alone were mostly recovered in the supernatant (Figure 9D, lanes 2 and 12). When mixed together, FH1-FH2-Cter induced the sedimentation of actin filaments in a concentration-dependent manner, consistent with bundle formation (Figure 9D, lanes 3 to 10). The bundling activity of FH1-FH2-Cter was independent of the presence of GST because the His-FH1-FH2-Cter-His fusion protein has a similar activity (Figure 9E, GST-FH1-FH2-Cter, open squares; His-FH1-FH2-Cter-His, closed squares) but depends strongly on the ionic strength (data not shown). AFH1 is a more efficient actin filament bundler than VILLIN1 (Figure 9E, closed circles; Huang et al., 2005). A possible explanation for the strong bundling activity of FH1-FH2-Cter comes from the strong affinity of FH1-FH2-Cter for the side of actin filaments (K_d ~0.13 μM; Figure 9E, inset), which is eightfold higher than VILLIN1 (K_d ~1 μM; Huang et al., 2005). In the same low-speed sedimentation assay, FH2-Cter has a weak actin bundling activity (Figure 9E, open circles), suggesting that the FH1 domain is essential for efficient bundle formation.

We used a light scattering assay to study the kinetics of bundle formation during actin polymerization (Huang et al., 2005; Figure 9F). Increasing the concentration of FH1-FH2-Cter induced a large increase in the amplitude of the polymerization curves, characteristic of bundle formation. For example, compare the

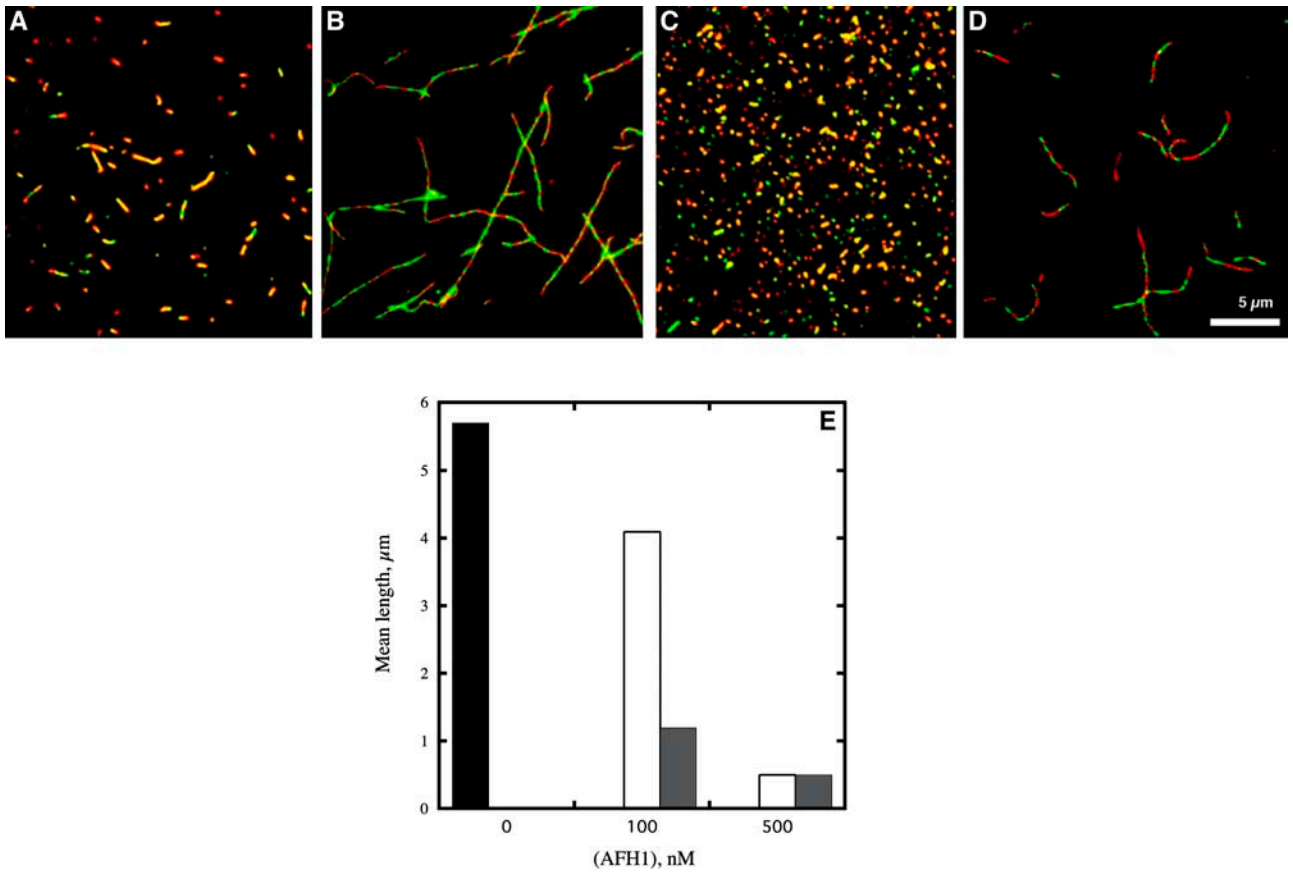

Figure 7. AFH1 Inhibits End-to-End Annealing of Actin Filaments.

Conditions: equal amounts of 2 μM rhodamine-phalloidin labeled actin filaments and Alexa green-phalloidin labeled actin filaments were mixed and sheared by sonication and then allowed to anneal for 10 min before dilution.
(A) Fragmented filaments imaged immediately.
(B) Fragmented filaments imaged after 10 min.
(C) Fragmented filaments in the presence of 100 nM FH2-Cter imaged after 10 min.
(D) Fragmented filaments in the presence of 100 nM FH1-FH2-Cter imaged after 10 min. Bar = 5 μm.
(E) Mean length distribution of fragmented filaments imaged at 10 min as a function of AFH1 concentrations. No AFH1, black bar; FH2-Cter, gray bars; FH1-FH2-Cter, white bars.

amplitude at 100 nM FH1-FH2-Cter (Figure 9F, closed circles) with the amplitude at 200 nM FH1-FH2-Cter (Figure 9F, open circles). The light scattering curves (Figure 9F) reached a plateau over a time frame comparable to the pyrene fluorescence curves (Figure 2B), suggesting that bundles form rapidly during polymerization. We also tested whether FH1-FH2-Cter was able to bundle preformed actin filaments (Figure 9G). Addition of FH1-FH2-Cter to actin filaments induced a rapid and large increase in light scattering, indicative of bundle formation (Figure 9E).

DISCUSSION

Here, we study in detail the mechanism of action of AFH1. Arabidopsis FORMINs comprise a large family of 21 isoforms separated into two classes according to the presence or absence of a predicted N-terminal transmembrane domain (Cvrcková, 2000; Deeks et al., 2002; Cvrcková et al., 2004). Formins are recently discovered actin nucleators responsible for actin cable formation in yeast (Evangelista et al., 1997; Pruyne et al., 2002; Sagot et al., 2002b). A general feature of nonplant formins is the presence of an actin nucleation domain (i.e., FH2 domain) and a polyproline-rich profilin binding domain (i.e., FH1 domain) (Evangelista et al., 2002). Arabidopsis class I formins seem to have retained this overall organization, whereas some divergence occurs in the class II FORMINs (Cvrcková, 2000; Deeks et al., 2002; Cvrcková et al., 2004). Although AFH1 is a member of Arabidopsis FORMIN class I, we found that it has a unique mode of action on actin polymerization. We show that a member of the formin family is able to generate actin bundles directly. Moreover, both the nucleating and the bundling activities of AFH1 depend on the Pro-rich FH1 domain that modulates the activity of the conserved FH2 nucleation domain. Indeed, the presence of FH1 domain converts the FH2 domain from a strong capper that

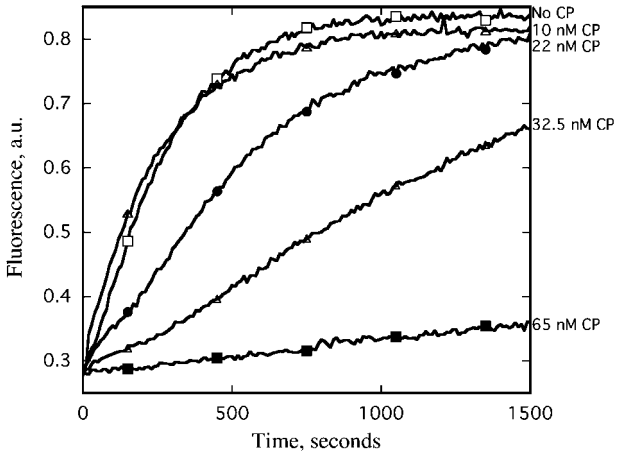

Figure 8. Arabidopsis CP Inhibits Nucleation by FH1-FH2-Cter.

Conditions: 10 mM imidazole-HCl, pH 7.0, 50 mM KCl, 2 mM $MgCl_2$, 1 mM EGTA, 0.2 mM ATP, 0.2 mM $CaCl_2$, 0.5 mM DTT, and 3 mM NaN_3 at 20°C. Actin (2 μM), profilin (2 μM), and FH1-FH2-Cter (65 nM) were incubated with various concentrations of CP before polymerization. The effect of increasing concentrations of Arabidopsis CP on actin polymerization in the presence of FH1-FH2-Cter and profilin monitored by pyrene fluorescence as a function of time is plotted.

blocks elongation at the barbed ends to a leaky capper that allows filament barbed-end growth. To decipher the contribution of proteins with multiple competing or synergistic effects on actin dynamics (including nucleation, capping, and bundling activities), we employed assays, including spectroscopy of pyrene fluorescence or light scattering, in parallel with fluorescence light microscopy by evanescent wave imaging of dynamic actin polymerization. The finding that AFH1 is not a simple actin nucleator but can generate actin bundles in vitro provides a potential explanation for the recent in vivo observation of actin cable formation induced by the overexpression of AFH1 in pollen tubes (Cheung and Wu, 2004).

Understanding how actin filaments are generated in plant cells remains an open question. The presence of high concentrations of profilin has been proposed to buffer the majority of free actin monomers (Gibbon et al., 1999; Staiger and Hussey, 2004). An important consequence of the high profilin concentration in vivo is the total inhibition of the spontaneous actin polymerization (Pollard et al., 2000). The in vivo polymerization of actin in a plant cell will therefore require regulation of the profilin–actin interaction or intervention of an actin nucleation factor. Analysis of the Arabidopsis genome reveals the presence of two universal homologs of actin nucleation-promoting factors, the Arp2/3 complex and FORMINs, although nucleating activity remains to be shown for the Arp2/3 complex (Cvrcková, 2000; Deeks et al., 2002; Deeks and Hussey, 2003; Cvrcková et al., 2004; Smith and Li, 2004; Wasteneys and Yang, 2004). Recently, a recombinant FH1-FH2-Cter fusion protein from AtFH5 was shown to nucleate actin filaments, whereas the FH2-Cter had no such activity (Ingouff et al., 2005). Here, we show that AFH1, FH1-FH2-Cter and FH2-Cter fusion proteins reduced the initial lag phase of the actin polymerization curves, corresponding to the nucleation step, in a concentration-dependent manner (Figures 2A and 2B). Fluorescence light microscopy provided further evidence of the nucleation efficiency for both AFH1 constructs. Indeed, the presence of AFH1 in the polymerization mixture reduced the length of actin filaments dramatically (Figures 2C to 2E). Because no severing activity for either AFH1 protein was detected, the decrease in actin filament length is best explained by an increase in the concentration of nuclei generated by AFH1, as reported previously for nucleation by the Acanthamoeba or mammalian Arp2/3 complex or other formins (Blanchoin et al., 2000b; Kovar et al., 2003). Both FH2-Cter and FH1-FH2-Cter constructs were able to nucleate actin alone, whereas the presence of the FH1 domain was essential for nucleation of the profilin/actin complex (Figure 3) and is in agreement with previous reports (Sagot et al., 2002b; Kovar et al., 2003; Pring et al., 2003; Romero et al., 2004). Moreover, FH2-Cter inhibits completely the polymerization of profilin/actin complex (Figure 3A) similar to other formins (Romero et al., 2004). Although similar data have been previously reported for other formins, additional data presented in this study suggest a mechanism of action for AFH1 that is different.

We find that both FH2-Cter and FH1-FH2-Cter bind to the barbed end of actin filaments, decrease the elongation rate of actin filaments, and inhibit end-to-end annealing of actin filaments. These properties, originally described for CPs (Andrianantoandro et al., 2001; Huang et al., 2003), have been extended to other proteins that interact with the barbed end of actin filaments, including formin and gelsolin (Kovar et al., 2003; Harris et al., 2004; Huang et al., 2004). The interaction of AFH1 with the barbed end of actin filaments is strongly dependent on the presence of the FH1 domain. We find that AFH1, FH2-Cter behaves similarly to Arabidopsis CP to block barbed-end elongation and allow nucleation of actin filaments that grow only from their pointed ends (Figures 3 to 7; Huang et al., 2003). Recently, the crystal structure of the yeast Bni1p FH2 domain in complex with tetramethylrhodamine-actin was solved (Otomo et al., 2005). This structure indicates that the barbed ends of actin filaments generated by FH2 are sterically blocked in agreement with our data (Otomo et al., 2005). However, Bni1p FH2 or FH1-FH2 domains nucleate filaments that elongate at their barbed ends (Pruyne et al., 2002; Sagot et al., 2002b; Kovar and Pollard, 2004a; Moseley et al., 2004). A possible explanation for this discrepancy, proposed by Otomo et al. (2005), is that the FH2 is in equilibrium between two states allowing or not allowing barbed-end growth. Our data suggest that the AFH1, FH2-Cter domain, like fission yeast Cdc12p, exists mostly in the state that sterically blocks barbed-end elongation (this study; Kovar et al., 2003). In contrast with Cdc12p, we report that AFH1, FH1-FH2-Cter binds to the barbed ends but still allows elongation at the same ends, in agreement with the leaky capping property previously reported for Bni1p (Figures 5 and 6; Zigmond et al., 2003). We propose that the presence of the FH1 domain in AFH1 induces a conformational change in the FH2 domain and stabilizes an accessible configuration at the barbed ends, making elongation at that end possible. This is closely related to the mechanism of action of fission yeast Cdc12 (FH1-FH2)p; however, Cdc12 (FH1-FH2)p alone is not sufficient to generate filaments that grow in the barbed-end direction and requires the presence of profilin bound to the FH1 domain (Kovar et al., 2003).

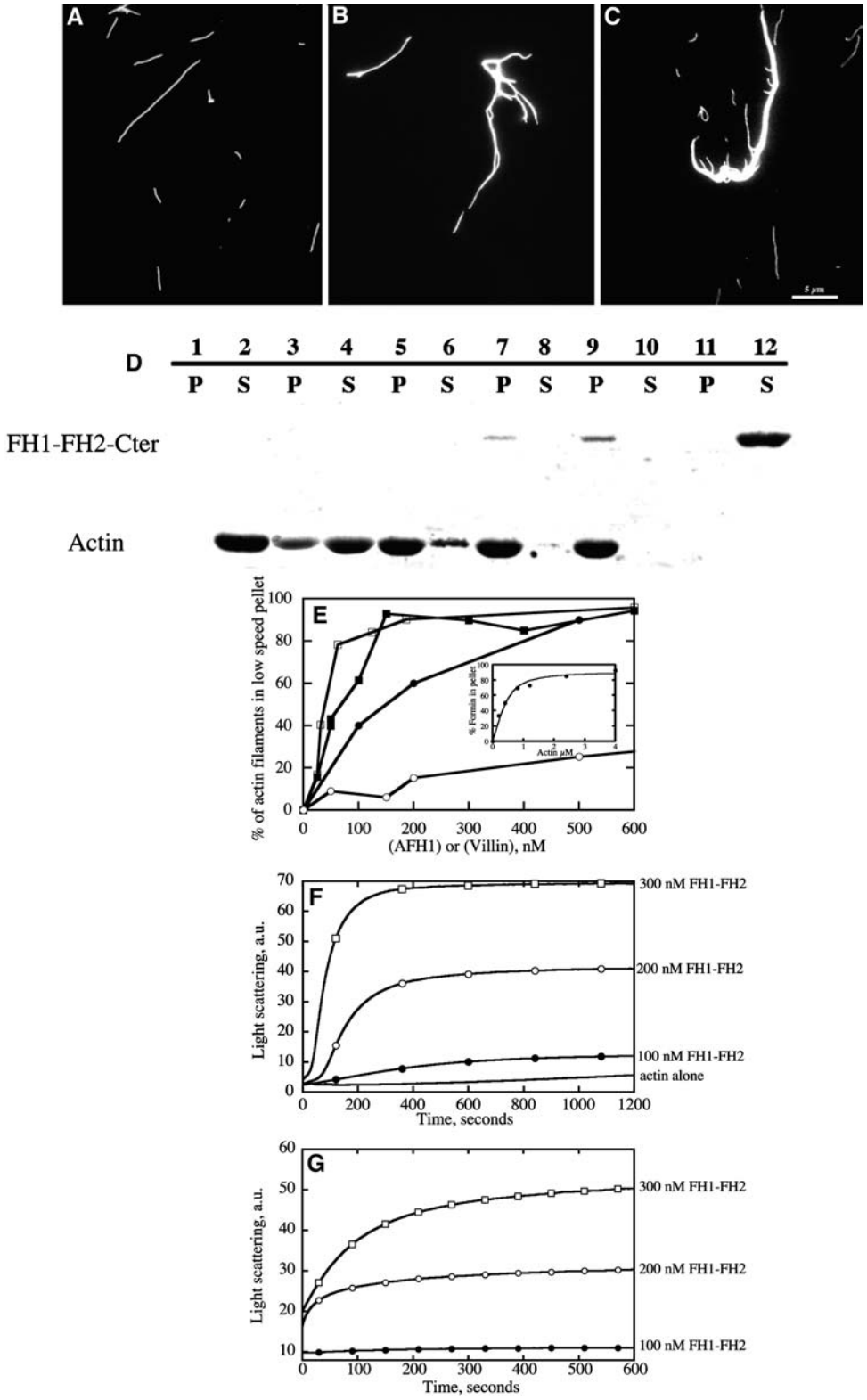

Figure 9. FH1-FH2-Cter but Not FH2-Cter Induced the Formation of Actin Bundles.

(A) to **(C)** Direct visualization of actin filament bundles in the presence of AFH1 or VILLIN1.
(A) Micrograph of actin filaments alone.

An attractive model for the behavior of AFH1 (FH1-FH2) can be extrapolated from the end-side binding model for mammalian formin proposed by Harris and Higgs (2004). In this model, the FH2 domain of formin binds to the side of actin subunits at the filament barbed ends (Harris and Higgs, 2004). In the case of AFH1, we propose that the FH2 domain alone binds mostly to the barbed ends of actin filaments, whereas the presence of the FH1 domain will induce a conformational change on AFH1 that allows a rapid equilibrium between the side binding and the end binding of the FH2-Cter domain, thereby allowing the switch from pointed-end to barbed-end elongation. This may explain why no actin filament buckling was observed between AFH1 (FH1-FH2) and myosin attachment points in the TIRF microscopy assay (Figures 5I to 5L), in contrast with findings with Cdc12p or Bni1p (Kovar and Pollard, 2004a). These data suggest that AFH1 (FH1-FH2) does not stay continuously bound to the growing barbed end. Obviously, this is not the only model possible. AFH1 (FH1-FH2) could also cycle rapidly on and off the barbed end of actin filaments to allow barbed-end growth. Based on the recent crystal structure of Bni1p FH2 bound to rhodamine actin (Otomo et al., 2005), we cannot predict the effect of the presence of the FH1 on the overall structure of formin bound to actin. The amino acid sequences of formin are divergent enough to allow major structural differences in their contacts with actin. Further structural information on the binding of AFH1 to actin will be required to fully understand the overall conformational change between FH2 and FH1-FH2 constructs.

The control of actin elongation at the barbed ends of actin filaments relies on tightly coordinated action of formin and CPs (Wear and Cooper, 2004). A conserved property of formin is to decrease the affinity of CP for the barbed end of actin filaments (Kovar et al., 2003; Zigmond et al., 2003; Harris et al., 2004; Moseley et al., 2004). Recently, Romero et al. (2004) demonstrated that the presence of formin (mDia1) lowers the affinity of CapG for the barbed ends by 100-fold. Interestingly, the binding of mDia1 and CapG to the barbed ends seems not to be directly competitive, but rather they form a complex that poisons actin elongation (Romero et al., 2004). We report that Arabidopsis CP, at a one-to-one molar ratio with FORMIN, inhibits actin polymerization induced by AFH1 (FH1-FH2) completely (Figure 8). This property, different from nonplant formins, favors a model whereby AFH1 (FH1-FH2) does not stay attached continuously at the barbed ends of actin filaments. So, the cellular concentrations of CP and formin, and their respective affinities for barbed ends, are key elements to understand how these two proteins will exert control over actin elongation. The affinity of Arabidopsis CP for the barbed ends of actin filament ($K_d \sim 12$ to 24 nM) is 6- to 100-fold lower than yeast or vertebrate CP (Huang et al., 2003). However, this affinity is only slightly affected by the presence of AFH1 (FH1-FH2) (data not shown). In plants, because of the lower affinity of CP for barbed ends, the inhibition by formin of barbed-end capping with CP may not be as relevant as in other organisms. Other cellular factors, including phosphatidylinositol 4,5-biphosphate (Huang et al., 2003) and phosphatidic acid (S. Huang, L.Y. Gao, L. Blanchoin, and C.J. Staiger, unpublished data), affect the activity of Arabidopsis CP and may play an important role in coordinating the dynamics at actin filament barbed ends in the presence of both formin and CPs.

An exciting novel feature of AFH1 (FH1-FH2) is the ability to bind the side of actin filaments and organize them into cable-like structures without a need for other cellular factors (Figure 9). We find that the FH1 domain is necessary for bundling by AFH1 (Figure 9). Bundling occurs during polymerization or on preformed actin filaments as revealed by a combination of fluorescence microscopy, low-speed sedimentation assays, and light scattering (Figure 9). This bundling activity is consistent with the end-side binding model because actin filament cross-linking requires an interaction with the side of actin filaments (this report; Harris and Higgs, 2004). Our data suggest that the capping, end binding site, and the bundling side binding site of AFH1 are tightly related. In the leaky capper state, the FH2 domain may bind to the barbed ends and to the side of actin filaments in a similar way. Indeed, the high affinity of FH1-FH2 for the side of actin filaments suggests that the majority of the cross-linking formin molecules will not be attached to the end of the filament (Figure 9). The bundling activity of AFH1 (FH1-FH2) is in good agreement with the effect of overexpression of AFH1 in pollen tubes (Cheung and Wu, 2004). Overexpression of AFH1 induces abundant actin cable formation and affects both the morphology and growth of the pollen tube (Cheung and Wu, 2004).

Actin cables have been reported to serve as tracks for vesicle delivery and are required for plasma membrane expansion and cell wall biogenesis (Shimmen and Yokota, 2004). This study emphasizes the potential role of formin in generation of actin-based structures in vivo. The localization of AFH1 depends on the putative N-terminal transmembrane domain, whereas its

Figure 9. (continued).

(B) Micrograph of actin filament bundles formed in the presence of 1 μM VILLIN1.

(C) Micrograph of actin filament bundles in the presence of 800 nM FH1-FH2-Cter. Bar = 5 μm.

(D) Bundling activity of FH1-FH2-Cter was determined by a low-speed cosedimentation assay. Lanes 1 and 2, actin filaments alone (2 μM); lanes 3 and 4, actin filaments and FH1-FH2-Cter (25 nM); lanes 5 and 6, actin filaments and 65 nM FH1-FH2-Cter; lanes 7 and 8, actin filaments and 125 nM FH1-FH2-Cter; lanes 9 and 10, actin filaments and 180 nM FH1-FH2-Cter; lanes 11 and 12, AFH1 alone at 500 nM. P, pellet; S, supernatant.

(E) Percentage of actin filaments recovered in the low-speed pellet as a function of the concentration of FH2-Cter (open circles), FH1-FH2-Cter protein (open squares), His-FH1-FH2-Cter-His (closed squares), or VILLIN1 (closed circles). Inset shows the percentage of FH1-FH2-Cter construct in the pellet as a function of actin filament concentration. FH1-FH2-Cter binds to actin filaments with an apparent K_d of 0.13 μM.

(F) Time course of actin polymerization monitored by light scattering. Actin alone, solid line; addition of FH1-FH2-Cter at 100 nM, closed circles; 200 nM, open circles; 300 nM, open squares.

(G) Time course of the increase in light scattering after addition of FH1-FH2-Cter to actin filaments. Actin filaments after addition of FH1-FH2-Cter at 100 nM closed circles; 200 nM, open circles; 300 nM, open squares.

activity lies in the FH1-FH2-Cter domains (Cheung and Wu, 2004; this study). However, AFH1 localization seems not restricted to the cell membrane (Cheung and Wu, 2004). Overexpression of the FH2 domain of AFH1 has a reduced activity with respect to the amount of actin cables present in the pollen tube (Cheung and Wu, 2004). Our study shows that AFH1, FH2-Cter and FH1-FH2-Cter domains have opposite effects on actin polymerization in the presence of profilin (Figure 3). FH1-FH2-Cter acts as a potent nucleator that rapidly generates new actin filaments from the profilin actin pool, whereas FH2-Cter acts as a strong actin filament barbed-end cap under the same conditions. Our data explain how the presence of profilin and the FH1 domain of AFH1 can modulate the function of this protein in agreement with the in vivo observations. Moreover, we have shown that FH1-FH2-Cter was able to generate actin bundles during polymerization or from preexisting filaments. Overexpression of FH1-FH2-Cter in pollen will reorganize all actin filaments into bundles independently of the nucleation activity. This activity is similar to other actin-bundling proteins, including plant fimbrin and villin (Kovar et al., 2000b; Huang et al., 2005; L.Y. Gao, D.W. McCurdy, and C.J. Staiger, unpublished data). Our data highlight the need for a careful characterization of the mechanism of action of actin binding proteins to further understand their in vivo functions. In a cellular context, we propose that AFH1 will initiate the formation of actin cable-like structures at the plasma membrane. The side binding and bundling activity of AFH1 could be important to initiate a cluster of actin cables in a very specific area. Obviously, depending on the context, these cables could be further stabilized by villin or other bundling proteins (Huang et al., 2005), or they could rapidly turnover by action of actin depolymerizing factor (ADF)/cofilin or gelsolin family members (Carlier et al., 1997; Maciver and Hussey, 2002; Huang et al., 2004). Localization of AFH1 with isoform-specific antibodies will be needed to further address the link between AFH1 and actin filament distribution in vivo.

FORMIN is a large family of 21 isoforms in Arabidopsis, separated into two classes depending on the presence of a transmembrane domain at the N terminus (Deeks et al., 2002; Cvrcková et al., 2004). There is no doubt that significant differences in the mechanism of action together with cellular localization of these formins will correlate with specific functions. Recently, Arabidopsis FORMIN5, AtFH5, a conserved actin nucleator, has been shown to affect cytokinesis and morphogenesis in endosperm (Ingouff et al., 2005). Another class I FORMIN, AtFH6, has been shown to be upregulated during parasitic nematode infection, but the mechanism involved in this regulation is largely unknown (Favery et al., 2004). It is highly ambitious just from the sequence to predict how a protein with the complexity of a formin will impact actin polymerization. Indeed, all formins tested so far present divergent properties (Kovar and Pollard, 2004b). Structural information is limited to the FH2 domain from yeast and mammalian formins (Shimada et al., 2004; Xu et al., 2004; Otomo et al., 2005) that are weakly conserved with plant formins, thereby preventing any solid prediction of the structure of the plant FH2 domain. The current view that the role of formin in vivo is to block barbed-end capping by CP and allow long actin cables to elongate is over simplified. We have shown that AFH1 is more than just a nucleator. Other cellular factors including ADF and villin, together with the bundling activity of AFH1, will strongly affect actin cable formation (Huang et al., 2005). Further work is needed to reveal if the bundling activity is a general feature of Arabidopsis FORMINs. Moreover, the amino acid sequence of AFH1 does not reveal any obvious mode for regulation of its activity. The degree of complexity of formin both as a multifunctional protein and as a large gene family will require concerted effort by the plant cytoskeleton community to understand their broad function. In any case, the fact that Arabidopsis plants defective for the Arp2/3 complex (the other conserved actin nucleator) have only minor phenotypes argues in favor of key functions played by FORMIN family proteins in plants.

METHODS

Protein Production

Two *AFH1* (At3g25500) fragments, FH1-FH2-Cter and FH2-Cter, were amplified by PCR from a RAFL clone containing *AFH1* cDNA (pda07914, RIKEN BioResource Center, Ibarabi, Japan) using *Not*I-6HisR, containing a 6-His tag (5′-ATAGTTTAGCGGCCGCCTAATGGTGATGGTGATGGTGG-TAAGAAACTAATGAGATTGAGTTATGTTCGTCTTCATC-3′) with *Sal*I-FH1 (5′-ACGCGTCGACGTCGGCAAGGTTTGCAATCTCAGTTA-3′) or *Sal*I-FH2 (5′-ACGCGTCGACGGTCTGAAAACTTACCAGTGACTTCG-3′) primers. Error-free *Sal*I-*Not*I PCR fragments were ligated to pGEX-4T1 vector (Amersham, Buckinghamshire, UK) restricted with *Sal*I-*Not*I. The fragment corresponding to the FH1-FH2-Cter construct was also inserted into pET30a vector (Novagen, Madison, WI) restricted with *Sal*I-*Not*I. These constructs were overexpressed in Rosetta Blue (DE3) pLysS strain of *Escherichia coli* (Novagen). Cells were grown to an OD_{600} of 0.8 at 37°C and induced with 0.5 mM isopropylthio-β-galactoside at 22°C overnight. Cultures were resuspended in extraction buffer (25 mM Tris-HCl, pH 7.5, 250 mM sodium chloride, 5% glycerol, 0.1% Triton X-100, 1 mM EDTA, and 1 mM DTT) with protease inhibitor cocktail. After sonication and centrifugation (23,000*g*, 30 min), the supernatant was incubated with glutathione-Sepharose 4B resin (Amersham), washed with TBSE (25 mM Tris-HCl, pH 8.0, 250 mM potassium chloride, 1 mM EDTA, and 1 mM DTT), and eluted with 100 mM glutathione in TBSE. Eluted fractions were dialyzed overnight against His purification buffer (25 mM Tris-HCl, pH 8.0, 250 mM potassium chloride, 5 mM imidazole, and 2 mM 2-mercaptoethanol). The dialyzed proteins were incubated for 1 h with Talon resin (Clontech, Palo Alto, CA), washed with buffer 2 (25 mM Tris-HCl, pH 8.0, 250 mM potassium chloride, 20 mM imidazole, and 2 mM 2-mercaptoethanol), and eluted with elution buffer (25 mM Tris-HCl, pH 8.0, 250 mM potassium chloride, 600 mM imidazole, and 2 mM 2-mercaptoethanol). After overnight dialysis against 25 mM Tris-HCl, pH 8.0, 150 mM potassium chloride, 1 mM EDTA, 1 mM DTT, and 1 mM sodium azide, proteins were concentrated with Centriprep YM-30 (Amicon, Bedford, MA) and flash frozen in liquid nitrogen. The His-FH1-FH2-Cter-His construct was purified using the same protocol without the glutathione-Sepharose step and dialyzed overnight in 25 mM imidazole, pH 8.0, 150 mM potassium chloride, 1 mM EDTA, 1 mM DTT, and 1 mM sodium azide.

Actin was isolated from rabbit skeletal muscle acetone powder (Spudich and Watt, 1971). Monomeric Ca-ATP-actin was purified by gel filtration chromatography on Sephacryl S-300 (MacLean-Fletcher and Pollard, 1980) at 4°C in G buffer (5 mM Tris-HCl, pH 8.0, 0.2 mM ATP, 0.1 mM $CaCl_2$, and 0.5 mM DTT). Actin was labeled on Cys-374 to a stoichiometry of 0.8 to 1.0 with pyrene iodoacetamide (Kouyama and Mihashi, 1981); as modified by Pollard (1984). Mg-ATP-actin was prepared by incubation of Ca-ATP-actin on ice with 0.2 mM EGTA and an 11-fold molar excess of $MgCl_2$ over actin and used within 1 h. Actin was polymerized by addition of one-tenth volume (v/v) of 10× KMEI (500 mM KCl, 10 mM $MgCl_2$, 10 mM EGTA, and 100 mM imidazole-HCl, pH 7.0).

Maize (*Zea mays*) pollen actin was purified according to Ren et al. (1997). *Arabidopsis thaliana* CP, human profilin 1, and maize PROFILIN5 (ZmPRO5) were purified as described previously (Fedorov et al., 1994; Carlier et al., 1997; Kovar et al., 2000a; Huang et al., 2003). If not stipulated, all experiments were performed with skeletal muscle actin and human profilin 1.

Actin Nucleation Assay

Actin nucleation was performed essentially as described by Higgs et al. (1999). Mg-ATP-monomeric actin or actin-profilin complexes (10% pyrene labeled) were polymerized at room temperature in the presence or absence of AFH1 by the addition of one-tenth volume of 10× KMEI. The polymerization was followed by changes in pyrene fluorescence using a MOS450 Bio-Logic fluorimeter (Bio-Logic-Science Instruments, Claix, France) or a Xenius SAFAS (Safas, Monaco).

Elongation Assay to Determine the Affinity of FH2-Cter and FH1-FH2-Cter for the Barbed End of Actin Filament

Equivalent amounts of actin filaments were incubated for a few minutes at room temperature with various concentrations of AFH1. Elongation was initiated by the addition of pyrene-labeled actin monomers or pyrene-labeled actin monomers bound to profilin to the actin filament mixture. The affinity of the fusion proteins for the barbed end of actin filaments was determined by the variation of the initial rate of elongation as a function of the concentration of AFH1 using Equation 1:

$$V_i = V_{if} + (V_{ib} - V_{if}) \left(\frac{K_d + [\text{ends}] + [\text{AFH1}] - \sqrt{(K_d + [\text{ends}] + [\text{AFH1}])^2 - 4[\text{ends}][\text{AFH1}]}}{2[\text{ends}]} \right), \quad (1)$$

where V_i is the observed rate of elongation, V_{if} is the rate of elongation when all the barbed ends are free, V_{ib} is the rate of elongation when all the barbed ends are capped, [ends] is the concentration of barbed ends, and [AFH1] is the concentration of AFH1. The data were modeled by Kaleidagraph version 3.6 software (Synergy Software, Reading, PA).

Fluorescence Microscopy

Actin filaments labeled with fluorescent phalloidin were observed in vitro by epifluorescence illumination as previously reported (Blanchoin et al., 2000b). Actin alone, or together with AFH1, was polymerized at room temperature in 1× KMEI and labeled with an equimolar amount of rhodamine-phalloidin (Sigma-Aldrich, St. Louis, MO) during polymerization. The polymerized F-actin was diluted to 10 nM in fluorescence buffer containing 10 mM imidazole-HCl, pH 7.0, 50 mM KCl, 1 mM $MgCl_2$, 100 mM DTT, 100 μg/mL glucose oxidase, 15 mg/mL glucose, 20 μg/mL catalase, and 0.5% methylcellulose. A dilute sample of 3 μL was applied to a 22 × 22-mm cover slip coated with poly-L-Lys (0.01%). Actin filaments were observed by epifluorescence illumination with a Zeiss Axioplan microscope (Jena, Germany) equipped with a 63×, 1.4–numerical aperture Planapo objective, and digital images were collected with a Hamamatsu ORCA CCD camera (Hamamatsu Photonics, Hamamatsu City, Japan) using Axiovision software.

Dual Color Annealing Assay

Actin filaments (2 μM) labeled with fluorescent rhodamine-phalloidin and 2 μM of actin filaments labeled with fluorescent Alexa-488-phalloidin (Molecular Probes, Eugene, OR) were mixed together in the presence or absence of AFH1. The filaments were sheared by a quick sonication and allowed to anneal for 10 min before dilution into fluorescence buffer. Actin filaments were observed by epifluorescence illumination as described above.

TIRF Microscopy

We used methods recently described by Kovar and Pollard (2004a). Actin filaments were observed by TIRF illumination on an Olympus IX-71 inverted microscope equipped with a 60×, 1.45–numerical aperture Planapo objective (Melville, NY). The time course of actin polymerization was acquired at 5-s intervals with a Hamamatsu ORCA-EM-CCD camera (model C9100-12) using WASABI Imaging Software (version 1.4; Hamamatsu Photonics, Herrsching, Germany). Glass flow cells (Amann and Pollard, 2001) were coated with a mixture of 10 nM NEM-myosin alone or with FH2-Cter (500 nM) or FH1FH2-Cter (200 nM) for 1 min and washed with 1% BSA in fluorescence buffer. A mixture of 1 μM Mg-ATP rhodamine-actin monomers 40% labeled (Cytoskeleton, Denver, CO) bound to 2 μM of ZmPRO5 in fluorescence buffer was injected into the flow cells, and image acquisition began as soon as possible (typically 20 s after injection) for a 20-min period.

Elongation rates were determined by measuring filament lengths during actin filaments elongation with MetaMorph version 6.2r6 (Universal Imaging, Media, PA). Linear fits were made to the plots of length versus time, with the slope representing elongation rates. Rates were converted from $\mu m \cdot s^{-1}$ to subunits$\cdot s^{-1}$ using 333 actin monomers per micrometer.

Cc Determination

A range of concentrations of 5% pyrene-labeled Mg-ATP-actin was polymerized in 1× KMEI in the absence or presence of FH2-Cter (200 nM), FH1FH2-Cter (200 nM), AtCP (200 nM), or gelsolin (200 nM) for 17 h in the dark at room temperature. Fluorescence measurements were performed at room temperature using a Safas Xenius fluorimeter. Linear best fit of the data, plotted as arbitrary fluorescence units versus actin concentration, was used to determine the intercept with *x* axis.

Low- and High-Speed Cosedimentation Assays

Low-speed cosedimentation assays were used to examine the actin-bundling properties of FH2-Cter and FH1-FH2-Cter as previously reported for Arabidopsis FIMBRIN1 and VILLIN1 (Kovar et al., 2000b; Huang et al., 2005). All proteins were preclarified at 200,000*g* before each experiment. Various concentrations of FH2-Cter or FH1-FH2-Cter and actin filaments were incubated together and then centrifuged at 13,500*g* for 30 min at 4°C. Supernatants and pellets were collected and proteins were separated by SDS-PAGE. Coomassie Brilliant Blue–stained gels were digitized with a CanoScanLide 30 (Canon, Courbevoie, France), and the density of gel bands was quantified in the supernatant and pellet using NIH image.

High-speed cosedimentation assay was performed identically to the low-speed assay except that the proteins were centrifuged at 300,000*g* for 30 min at 20°C before separation of the supernatant and pellet.

Light Scattering Assay to Characterize Filament Bundling Activity

A kinetic light scattering assay was performed to determine the ability of FH1-FH2-Cter to form actin bundles. Light scattering was monitored by 90° light scattering of unlabeled actin at 400 nm. The change of light scattering was recorded after addition of various concentrations of AFH1 into 2 μM F-actin solution with a Safas Xenius fluorimeter.

ACKNOWLEDGMENTS

We thank Lisa Gao and Faisal Chaudhry for providing purified pollen actin and plant profilin, François Parcy for advice on the cloning of AFH1

with a 6-His tag, and Robert Robinson and Rajaa Paterski-Boujemaa for critical reading of the manuscript. We are grateful to Harry Higgs for sharing unpublished data. This work was funded through grants from the Actions Thèmatiques et Initiatives sur Programmes et Equipes to L.B. and from the National Research Initiative of the USDA Cooperative State Research, Education, and Extension Service (Grant 2002-35304-12412 to C.J.S.). The TIRF microscope facility was supported by a grant from the Bindley Bioscience Center at Purdue University.

Received January 15, 2005; revised May 16, 2005; accepted May 19, 2005; published July 1, 2005.

REFERENCES

Amann, K.J., and Pollard, T.D. (2001). Direct real-time observation of actin filament branching mediated by Arp2/3 complex using total internal reflection fluorescence microscopy. Proc. Natl. Acad. Sci. USA **981,** 15009–15013.

Andrianantoandro, E., Blanchoin, L., Sept, D., McCammon, J.A., and Pollard, T.D. (2001). Kinetic mechanism of end-to-end annealing of actin filaments. J. Mol. Biol. **312,** 721–730.

Banno, H., and Chua, N.H. (2000). Characterization of the *Arabidopsis* formin-like protein AFH1 and its interacting protein. Plant Cell Physiol. **41,** 617–626.

Blanchoin, L., Amann, K.J., Higgs, H.N., Marchand, J.B., Kaiser, D.A., and Pollard, T.D. (2000b). Direct observation of dendritic actin filament networks nucleated by Arp2/3 complex and WASP/Scar proteins. Nature **404,** 1007–1011.

Blanchoin, L., Pollard, T.D., and Mullins, R.D. (2000a). Interaction of ADF/cofilin, Arp2/3 complex, capping protein and profilin in remodeling of branched actin filament networks. Curr. Biol. **10,** 1273–1282.

Carlier, M.F., Laurent, V., Santolini, J., Melki, R., Didry, D., Xia, G.X., Hong, Y., Chua, N.H., and Pantaloni, D. (1997). Actin depolymerizing factor (ADF/cofilin) enhances the rate of filament turnover: Implication in actin-based motility. J. Cell Biol. **136,** 1307–1322.

Chen, C.Y., Wong, E.I., Vidali, L., Estavillo, A., Hepler, P.K., Wu, H.M., and Cheung, A.Y. (2002). The regulation of actin organization by actin-depolymerizing factor in elongating pollen tubes. Plant Cell **14,** 2175–2190.

Cheung, A.Y., and Wu, H.M. (2004). Overexpression of an Arabidopsis formin stimulates supernumerary actin cable formation from pollen tube cell membrane. Plant Cell **16,** 257–269.

Cvrcková, F. (2000). Are plant formins integral membrane proteins? Genome Biol. **1,** 1–7.

Cvrcková, F., Novotny, M., Pickova, D., and Zársky, V. (2004). Formin homology 2 domains occur in multiple contexts in angiosperms. BMC Genomics **5,** 1–18.

Deeks, M.J., and Hussey, P.J. (2003). Arp2/3 and 'the shape of things to come'. Curr. Opin. Plant Biol. **6,** 561–567.

Deeks, M.J., Hussey, P.J., and Davies, B. (2002). Formins: Intermediates in signal-transduction cascades that affect cytoskeletal reorganization. Trends Plant Sci. **7,** 492–498.

Evangelista, M., Blundell, K., Longtine, M., Chow, C., Adames, N., Pringle, J., Peter, M., and Boone, C. (1997). Bni1p, a yeast formin linking cdc42p and the actin cytoskeleton during polarized morphogenesis. Science **276,** 118–122.

Evangelista, M., Pruyne, D., Amberg, D.C., Boone, C., and Bretscher, A. (2002). Formins direct Arp2/3-independent actin filament assembly to polarize cell growth in yeast. Nat. Cell Biol. **4,** 32–41.

Favery, B., Chelysheva, L.A., Lebris, M., Jammes, F., Marmagne, A., De Almeida-Engler, J., Lecomte, P., Vaury, C., Arkowitz, R.A., and Abad, P. (2004). Arabidopsis formin AtFH6 is a plasma membrane-associated protein upregulated in giant cells induced by parasitic nematodes. Plant Cell **16,** 2529–2540.

Fedorov, A.A., Pollard, T.D., and Almo, S.C. (1994). Purification, characterization and crystallization of human platelet profilin expressed in *Escherichia coli*. J. Mol. Biol. **241,** 480–482.

Feierbach, B., and Chang, F. (2001). Roles of the fission yeast formin for3p in cell polarity, actin cable formation and symmetric cell division. Curr. Biol. **11,** 1656–1665.

Gibbon, B.C., Kovar, D.R., and Staiger, C.J. (1999). Latrunculin B has different effects on pollen germination and tube growth. Plant Cell **11,** 2349–2363.

Gibbon, B.C., Ren, H., and Staiger, C.J. (1997). Characterization of maize (*Zea mays*) pollen profilin function in vitro and in live cells. Biochem. J. **327,** 909–915.

Harris, E.S., and Higgs, H.N. (2004). Actin cytoskeleton: Formins lead the way. Curr. Biol. **14,** R520–R522.

Harris, E.S., Li, F., and Higgs, H.N. (2004). The mouse formin, FRLalpha, slows actin filament barbed end elongation, competes with capping protein, accelerates polymerization from monomers, and severs filaments. J. Biol. Chem. **279,** 20076–20087.

Hepler, P.K., Vidali, L., and Cheung, A.Y. (2001). Polarized cell growth in higher plants. Annu. Rev. Cell Dev. Biol. **17,** 159–187.

Higashida, C., Miyoshi, T., Fujita, A., Oceguera-Yanez, F., Monypenny, J., Andou, Y., Narumiya, S., and Watanabe, N. (2004). Actin polymerization-driven molecular movement of mDia1 in living cells. Science **303,** 2007–2010.

Higgs, H.N., Blanchoin, L., and Pollard, T.D. (1999). Influence of the Wiskott-Aldrich syndrome protein (WASp) C terminus and Arp2/3 complex on actin polymerization. Biochemistry **38,** 15212–15222.

Holdaway-Clarke, T.L., and Hepler, P.K. (2003). Control of pollen tube growth. New Phytol. **159,** 539–563.

Huang, S., Blanchoin, L., Chaudhry, F., Franklin-Tong, V.E., and Staiger, C.J. (2004). A gelsolin-like protein from *Papaver rhoeas* pollen (PrABP80) stimulates calcium-regulated severing and depolymerization of actin filaments. J. Biol. Chem. **279,** 23364–23375.

Huang, S., Blanchoin, L., Kovar, D.R., and Staiger, C.J. (2003). Arabidopsis capping protein (AtCP) is a heterodimer that regulates assembly at the barbed ends of actin filaments. J. Biol. Chem. **278,** 44832–44842.

Huang, S., Robinson, R.C., Gao, L.Y., Matsumoto, T., Brunet, A., Blanchoin, L., and Staiger, C.J. (2005). Arabidopsis VILLIN1 generates actin filament cables that are resistant to depolymerization. Plant Cell **17,** 486–501.

Ingouff, M., Fitz Gerald, J.N., Guérin, C., Robert, H., Sørensen, M.B., Van Damme, D., Geelen, D., Blanchoin, L., and Berger, F. (2005). Plant formin AtFH5 is an evolutionarily conserved actin nucleator in cytokinesis. Nat. Cell Biol. **7,** 374–380.

Kouyama, T., and Mihashi, K. (1981). Fluorimetry study of N-(1-pyrenyl) iodoacetamide-labelled F-actin. Local structural change of actin protomer both on polymerization and on binding of heavy meromyosin. Eur. J. Biochem. **114,** 33–38.

Kovar, D.R., Drobak, B.K., and Staiger, C.J. (2000a). Maize profilin isoforms are functionally distinct. Plant Cell **12,** 583–598.

Kovar, D.R., Kuhn, J.R., Tichy, A.L., and Pollard, T.D. (2003). The fission yeast cytokinesis formin Cdc12p is a barbed end actin filament capping protein gated by profilin. J. Cell Biol. **161,** 875–887.

Kovar, D.R., and Pollard, T.D. (2004a). Insertional assembly of actin filament barbed ends in association with formins produces piconewton forces. Proc. Natl. Acad. Sci. USA **101,** 14725–14730.

Kovar, D.R., and Pollard, T.D. (2004b). Progressing actin: Formin as a processive elongation machine. Nat. Cell Biol. **6,** 1158–1159.

Kovar, D.R., Staiger, C.J., Weaver, E.A., and McCurdy, D.W. (2000b). AtFim1 is an actin filament crosslinking protein from *Arabidopsis thaliana*. Plant J. **24,** 625–636.

Le, J., El-Assal Sel, D., Basu, D., Saad, M.E., and Szymanski, D.B. (2003). Requirements for Arabidopsis ATARP2 and ATARP3 during epidermal development. Curr. Biol. **13,** 1341–1347.

Li, F., and Higgs, H.N. (2003). The mouse Formin mDia1 is a potent actin nucleation factor regulated by autoinhibition. Curr. Biol. **13,** 1335–1340.

Li, Z., Kim, E.S., and Bearer, E.L. (2002). Arp2/3 complex is required for actin polymerization during platelet shape change. Blood **99,** 4466–4474.

Lin, Y., and Yang, Z. (1997). Inhibition of pollen tube elongation by microinjected anti-Rop1Ps antibodies suggests a crucial role for Rho-type GTPases in the control of tip growth. Plant Cell **9,** 1647–1659.

Machesky, L.M., Atkinson, S.J., Ampe, C., Vandekerckhove, J., and Pollard, T.D. (1994). Purification of a cortical complex containing two unconventional actins from *Acanthamoeba* by affinity chromatography on profilin agarose. J. Cell Biol. **127,** 107–115.

Maciver, S.K., and Hussey, P.J. (2002). The ADF/cofilin family: Actin-remodeling proteins. Genome Biol. **3**.

MacLean-Fletcher, S., and Pollard, T.D. (1980). Mechanism of action of cytochalasin B on actin. Cell **20,** 329–341.

Mathur, J., Mathur, N., Kernebeck, B., and Hulskamp, M. (2003a). Mutations in actin-related proteins 2 and 3 affect cell shape development in Arabidopsis. Plant Cell **15,** 1632–1645.

Mathur, J., Mathur, N., Kirik, V., Kernebeck, B., Srinivas, B.P., and Hulskamp, M. (2003b). Arabidopsis *CROOKED* encodes for the smallest subunit of the ARP2/3 complex and controls cell shape by region specific fine F-actin formation. Development **130,** 3137–3146.

Moseley, J.B., Sagot, I., Manning, A.L., Xu, Y., Eck, M.J., Pellman, D., and Goode, B.L. (2004). A conserved mechanism for Bni1- and mDia1-induced actin assembly and dual regulation of Bni1 by Bud6 and profilin. Mol. Biol. Cell **15,** 896–907.

Mullins, R.D., Heuser, J.A., and Pollard, T.D. (1998). The interaction of Arp2/3 complex with actin: Nucleation, high-affinity pointed end capping, and formation of branching networks of filaments. Proc. Natl. Acad. Sci. USA **95,** 6181–6186.

Otomo, T., Tomchick, D.R., Otomo, C., Panchal, S.C., Machius, M., and Rosen, M.K. (2005). Structural basis of actin filament nucleation and processive capping by a formin homology 2 domain. Nature **433**, 488–494.

Pollard, T.D. (1984). Polymerization of ADP-actin. J. Cell Biol. **99,** 769–777.

Pollard, T.D., Blanchoin, L., and Mullins, R.D. (2000). Molecular mechanisms controlling actin filament dynamics in nonmuscle cells. Annu. Rev. Biophys. Biomol. Struct. **29,** 545–576.

Pring, M., Evangelista, M., Boone, C., Yang, C., and Zigmond, S.H. (2003). Mechanism of formin-induced nucleation of actin filaments. Biochemistry **42,** 486–496.

Pruyne, D., Evangelista, M., Yang, C., Bi, E., Zigmond, S., Bretscher, A., and Boone, C. (2002). Role of formins in actin assembly: Nucleation and barbed-end association. Science **297,** 612–615.

Ren, H., Gibbon, B.C., Ashworth, S.L., Sherman, D.M., Yuan, M., and Staiger, C.J. (1997). Actin purified from maize pollen functions in living plant cells. Plant Cell **9,** 1445–1457.

Romero, S., Le Clainche, C., Didry, D., Egile, C., Pantaloni, D., and Carlier, M.F. (2004). Formin is a processive motor that requires profilin to accelerate actin assembly and associated ATP hydrolysis. Cell **119,** 419–429.

Sagot, I., Klee, S.K., and Pellman, D. (2002a). Yeast formins regulate cell polarity by controlling the assembly of actin cables. Nat. Cell Biol. **4,** 42–50.

Sagot, I., Rodal, A.A., Moseley, J., Goode, B.L., and Pellman, D. (2002b). An actin nucleation mechanism mediated by Bni1 and profilin. Nat. Cell Biol. **4,** 626–631.

Shimada, A., Nyitrai, M., Vetter, I.R., Kuhlmann, D., Bugyi, B., Narumiya, S., Geeves, M.A., and Wittinghofer, A. (2004). The core FH2 domain of diaphanous-related formins is an elongated actin binding protein that inhibits polymerization. Mol. Cell **13,** 511–522.

Shimmen, T., and Yokota, E. (2004). Cytoplasmic streaming in plants. Curr. Opin. Cell Biol. **16,** 68–72.

Smith, L.G., and Li, R. (2004). Actin polymerization: Riding the wave. Curr. Biol. **14,** R109–R111.

Snowman, B.N., Kovar, D.R., Shevchenko, G., Franklin-Tong, V.E., and Staiger, C.J. (2002). Signal-mediated depolymerization of actin in pollen during the self-incompatibility response. Plant Cell **14,** 2613–2626.

Spudich, J.A., and Watt, S. (1971). The regulation of rabbit skeletal muscle contraction. I. Biochemical studies of the interaction of the tropomyosin-troponin complex with actin and the proteolytic fragments of myosin. J. Biol. Chem. **246,** 4866–4871.

Staiger, C.J. (2000). Signaling to the actin cytoskeleton in plants. Annu. Rev. Plant Physiol. **51,** 257–288.

Staiger, C.J., and Hussey, P.J. (2004). Actin and actin-modulating proteins. In The Plant Cytoskeleton in Cell Differentiation and Development, P.J. Hussey, ed (Oxford: Blackwell Publishers), pp. 32–80.

Staiger, C.J., Yuan, M., Valenta, R., Shaw, P.J., Warn, R.M., and Lloyd, C.W. (1994). Microinjected profilin affects cytoplasmic streaming in plant cells by rapidly depolymerizing actin microfilaments. Curr. Biol. **4,** 215–219.

Szymanski, D.B., Marks, M.D., and Wick, S.M. (1999). Organized F-actin is essential for normal trichome morphogenesis in Arabidopsis. Plant Cell **11,** 2331–2347.

Van Damme, D., Bouget, F.Y., Van Poucke, K., Inze, D., and Geelen, D. (2004). Molecular dissection of plant cytokinesis and phragmoplast structure: A survey of GFP-tagged proteins. Plant J. **40,** 386–398.

Vantard, M., and Blanchoin, L. (2002). Actin polymerization processes in plant cells. Curr. Opin. Plant Biol. **5,** 502–506.

Vidali, L., McKenna, S.T., and Hepler, P.K. (2001). Actin polymerization is essential for pollen tube growth. Mol. Biol. Cell **12,** 2534–2545.

Wasteneys, G.O., and Galway, M.E. (2003). Remodeling the cytoskeleton for growth and form: An overview with some new views. Annu. Rev. Plant Biol. **54,** 691–722.

Wasteneys, G.O., and Yang, Z. (2004). New views on the plant cytoskeleton. Plant Physiol. **136,** 3884–3891.

Watanabe, N., Madaule, P., Reid, T., Ishizaki, T., Watanabe, G., Kakizuka, A., Saito, Y., Nakao, K., Jockusch, B., and Narumiya, S. (1997). p140mDia, a mammalian homolog of *Drosophila* diaphanous, is a target protein for Rho small GTPase and is a ligand for profilin. EMBO J. **16,** 3044–3056.

Wear, M.A., and Cooper, J.A. (2004). Capping protein: New insights into mechanism and regulation. Trends Biochem. Sci. **29,** 418–428.

Xu, Y., Moseley, J.B., Sagot, I., Poy, F., Pellman, D., Goode, B.L., and Eck, M.J. (2004). Crystal structures of a Formin Homology-2 domain reveal a tethered dimer architecture. Cell **116,** 711–723.

Yen, L.F., Liu, X., and Cai, S. (1995). Polymerization of actin from maize pollen. Plant Physiol. **107,** 73–76.

Zigmond, S.H., Evangelista, M., Boone, C., Yang, C., Dar, A.C., Sicheri, F., Forkey, J., and Pring, M. (2003). Formin leaky cap allows elongation in the presence of tight capping proteins. Curr. Biol. **13,** 1820–1823.